NASA CONTRACTOR REPORT

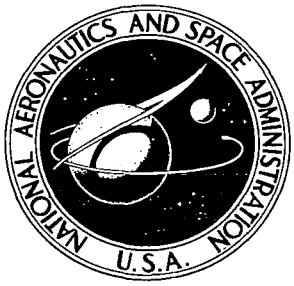

NASA CR-107

NASA CR-1071

INVESTIGATION OF WARM FOG PROPERTIES AND FOG MODIFICATION CONCEPTS

by Warren C. Kocmond and James E. Jiusto

Prepared by
CORNELL AERONAUTICAL LABORATORY, INC.
Buffalo, N. Y.
for

NATIONAL AERONAUTICS AND SPACE ADMINISTRATION • WASHINGTON, D. C. • JUNE 1968

NASA CR-1071

INVESTIGATION OF WARM FOG PROPERTIES AND FOG MODIFICATION CONCEPTS

By Warren C. Kocmond and James E. Jiusto

Issued by Originator as CAL Report No. RM-1788-P-17

Prepared under Contract No. NASr-156 by
CORNELL AERONAUTICAL LABORATORY, INC.
Buffalo, N.Y.

for

NATIONAL AERONAUTICS AND SPACE ADMINISTRATION

For sale by the Clearinghouse for Federal Scientific and Technical Information
Springfield, Virginia 22151 – CFSTI price $3.00

TABLE OF CONTENTS

TABLE OF CONTENTS (Cont'd.)

LIST OF FIGURES

LIST OF TABLES

ACKNOWLEDGMENTS

The authors are indebted to Mr. Roland J. Pilié for his contributions in preparing this document and for his many pertinent suggestions during the experimental and theoretical phases of the investigation.

Thanks are also due to Mr. Vito DePalma for his part in the design and testing of the particle classifier-disseminator; to Mr. George Zigrossi for his assistance in maintaining equipment and obtaining the data; and to Mr. Eugene Mack for analyzing much of the data.

ABSTRACT

Analytic and experimental investigations were conducted to examine the concept of modifying fog with hygroscopic material. The results indicate that it is possible to improve visibility in warm fog by seeding with micron-size salt particles (NaCl). The visibility in laboratory fog (produced in a 600 m^3 chamber) was increased by factors of three to ten, with as little as 1.7 mg of NaCl m^{-3} being effective. Only modest reductions (<1%) in ambient relative humidity were involved. Extrapolation of these results suggests that clearing a suitable landing zone for aircraft would not involve prohibitive amounts of seeding material. Recommendations are made for field testing the concept.

Laboratory experiments also suggest that the formation of fog can be modified by seeding the atmosphere with salt nuclei prior to fog formation. While visibility improvements of a factor of two were achieved in the laboratory, the concept appears less practical for field use.

An improved cloud nucleus chamber of the thermal gradient diffusion type was designed and is described together with results of a third year of observations. A "haze chamber" for measuring the concentrations of large and giant nuclei is discussed.

I. INTRODUCTION

The primary objective of Project Fog Drops is to investigate, both theoretically and experimentally, promising techniques for warm fog suppression and if possible, develop a practical method for improving visibility in dense natural fog. A necessary prerequisite for achieving this goal is a thorough understanding of basic fog properties and dynamics. During the first two years of research, physical and dynamic fog models were developed and experiments were conducted to determine more about the diffusional growth rates of droplets in a supersaturated environment. Observations were made of fog and cloud nucleus concentrations and studies were initiated to determine whether fog droplet coalescence or diffusional growth rates could be effectively enhanced. During the program's third year, emphasis was placed on obtaining measurements of physical characteristics of fog, learning more about the concentration and variability of cloud and fog nuclei and evaluating, on a laboratory scale, suggested concepts for fog suppression.

The work of the previous three contract periods was continued during the fourth year, with emphasis being placed on investigation of the concept for improving visibility in fog by seeding with hygroscopic nuclei of carefully controlled size. This concept was carefully examined, both theoretically and experimentally in a large laboratory chamber. Results of this work, which proved very promising, formed the basis for recommendations for a set of field experiments aimed at developing methods for dissipation of fog in a suitable landing zone at an airport.

II. SUMMARY

Program accomplishments for the first three years of research have been summarized in previous annual reports and, for brevity, will only be touched upon here. The accomplishments of the fourth year are discussed in some detail in part B of this section.

A. Program Accomplishments for Years I-III

Physical and dynamic fog models were formulated for radiation and advection fogs, as well as for steam fog. A fog climatology was established for the continental United States.

Theoretical and experimental investigations showed that droplet growth and evaporation rates can be decreased by treatment of the droplets with certain chemical monolayers. Further, we demonstrated that treatment of condensation nuclei with monolayers prior to droplet formation did not prevent activation of the nuclei, but did inhibit growth of droplets that formed on the nuclei. An effective means of treating droplets and/or nuclei in the free atmosphere, however, was not found. Ionic surfactants were shown to inhibit rather than promote droplet coalescence.

It was shown both theoretically and in the laboratory that it is impractical to attempt to modify fog by placing electrical charge on the droplets. We have therefore recommended that no further effort be devoted to fog suppression concepts based on artificial charging of droplets.

Using a thermal diffusion chamber developed on this program, daily measurements were made of the concentrations of cloud and fog nuclei active at slight supersaturations. This work was continued during year IV.

Industrial pollutants and other sources of contamination differ markedly in their ability to produce cloud and fog nuclei. Observations of cloud nuclei in urban and rural areas of New York and Pennsylvania and on the Island of Hawaii show that cloud nucleus concentrations in continental areas are one to two orders of magnitude greater than those in maritime

atmospheres. On the basis of our measurements, it appears that the supersaturation in natural fog rarely exceeds a few hundreths of a percent in continental areas since several hundred nuclei per cm^3 can generally be activated to fog drop sizes at these slight supersaturations.

A procedure for preventing dense natural fog from forming by seeding with hygroscopic nuclei of carefully controlled size was successfully demonstrated in small-scale laboratory experiments (8 cubic foot cloud chamber). Nuclei in the 2μ to 5μ radius range were selected as being optimum for the pre-seeding approach. Visibility improvements of up to a factor of two were achieved in these experiments. Using these results as a starting point, our attention turned toward evaluating this concept in the 600 m^3 chamber at the CAL Ordnance Laboratory in Ashford, New York. Results of these experiments, as well as other tests, are summarized in section II-B.

B. Program Accomplishments During Year IV

During preparation for the pre-seeding experiments in the 600 m^3 chamber, we considered a second set of experiments designed to suppress fog after it had formed. Preliminary calculations showed that seeding with a relatively few hygroscopic nuclei in the one to ten micron radius range would extract sufficient water from the atmosphere before falling through the chamber to cause evaporation of the natural fog droplets. With the new drop size distribution, consisting of a relatively few, large droplets, the scattering coefficient would be substantially smaller than that of the natural fog containing the same water. In addition, the larger droplets would precipitate more rapidly and further improve visibility.

Both sets of experiments were conducted in the 600 m^3 chamber. Results were extremely promising. The visibility in fog was consistently improved by factors ranging from three to ten by seeding with NaCl nuclei in concentrations as small as 1.7 mg m^{-3}.

On the basis of these results, it is recommended that field tests in fog be conducted during the coming year. We regard seeding after fog formation as being the more promising approach in practice since 1) significant increases in visibility can be obtained with relatively small amounts of material (perhaps as little as 100 kg to open a landing zone at an airport); 2) accurate fog prediction is not a prerequisite; and 3) the concept has more general applicability.

To produce nuclei of the right size for the seeding experiments, a unique particle classifier was developed on this program. The classifier is capable of producing 50 to 60 percent of the particles, by number, in the size range of 2μ to 5μ radius and 85 to 90 percent in the usable 1μ to 5μ range. A particularly important feature of this instrument is its ability to disseminate properly sized particles directly into the laboratory fog, thus eliminating natural fracture during storage of pre-sized particles and virtually eliminating agglomeration.

Related accomplishments during the fourth year included the design and development of a haze chamber, which is a chemical-thermal diffusion chamber suitable for making observations of fog and cloud nuclei at sub-saturated humidities. From these measurements, more should be learned about the concentration of large ($0.1 < r < 1.0\mu$) and giant ($r > 1.0\mu$) nuclei that are responsible for the initial stages of fog formation.

Cloud nucleus observations were also made on a routine basis throughout the fourth year. The data accumulated during the past three years represents one of the most complete records of cloud nucleus concentrations in existence.

III. TECHNICAL DISCUSSION

The initial plan for Year IV of this program was to concentrate on investigation of the pre-seeding concept aimed at preventing the formation of dense radiation fog. We planned to supply small concentrations of large hygroscopic nuclei to the atmosphere prior to fog formation. Calculations and preliminary experiments indicated that such nuclei could condense all of the water out of the atmosphere that was made available for fog formation. Thus, natural nuclei would not be activated and the fog would consist of a relatively few, large droplets. The scattering coefficient, or extinction coefficient, of a fog having such a drop-size distribution would be substantially smaller than that of a natural fog of the same liquid water content.

While preparing for large scale laboratory tests of the pre-seeding concept, we also considered the idea for suppressing fog that had already formed by seeding with hygroscopic nuclei. Rather than attempt to cause growth of very large droplets that precipitate rapidly and leave the atmosphere at substantially subsaturated relative humidities, which requires an excessive amount of seeding material, we aimed at modifying the drop-size distribution in such a way as to reduce the Mie scattering coefficient in order to improve visibility.

Since very rapid precipitation of droplets was not required, droplets formed on each hygroscopic nucleus could remain in the fog long enough to become highly diluted. By proper choice of size of the hygroscopic nuclei, each nucleus could account for the maximum mass of water, i.e. approach the molar concentration that would be in equilibrium with the vapor pressure of the surrounding atmosphere, before falling out. At the same time we sought the minimum total mass of nucleating material that would lower the ambient vapor pressure just enough to cause the desired redistribution of liquid water. After investigations indicated that this concept was promising, it was given primary attention on the program.

The calculations discussed in section III-A were performed to provide an estimate of the optimum particle size to be used in terms of total mass required, maximum visibility improvement to be achieved, and rate of visibility improvement. The results indicate that approximately five-micron radius particles are optimum, with particles as small as one-micron radius being useable in shallow fogs. The experiments discussed in section III-B demonstrate that it is possible to improve the visibility in existing laboratory fog by factors of three to ten by seeding with salt particles of these sizes. The calculations and experiments suggest that the mass of nucleating material required is sufficiently small to be feasible for use at airports.

Results of the pre-seeding experiments are reported in section III-C, while the investigation of natural atmospheric nuclei is discussed in section III-D.

A. Theory of Fog Modification Employing Giant Hygroscopic Nuclei

Over the years there has been periodic interest in the possibility of modifying fogs with hygroscopic materials. The usual intent has been to extract a portion of the water vapor in the saturated air so that evaporation of the fog droplets can occur.

The most notable and rigorous effort of this type - and one that achieved limited success - was performed by Houghton and Radford (1938). In their now classic work, which treated several aspects of the fog problem, clearing of modest size volumes (up to 10^6 m^3) was obtained by seeding with droplets of calcium chloride solution. The experiments were designed to reduce the ambient relative humidity to approximately 90% with clearing rates of 2000 m^3/sec. In general, solution spray rates of about 5 liters per second, or approximately 2.5 g of seeding material per cubic meter of fog, yielded the desired result.

Our approach has differed from the above in two respects:

1. dry salt particles (sodium chloride) of prescribed sizes are employed;

2. only slight reductions in ambient relative humidity are demanded, sufficient to alter the drop size distribution, enhance fallout, and to improve visibility above critical landing limits.

In principle, improvements in fog visibility can be effected by shifting the drop-size distribution to larger sizes or by decreasing the liquid water content of the fog. These conclusions can be drawn from a form of the visibility equation derived by Trabert (1901):

$$V = \frac{c}{\omega} \frac{\sum n_r r^3}{\sum n_r r^2} \simeq 2.6 k \frac{\overline{r}}{\omega} , \qquad (1)$$

where V is the visibility in a cloud, n_r the concentration of droplets of radius r, ω the liquid water content, c a numerical scattering factor (2.6), $\bar{r}$ the linear-mean droplet radius, and k an empirical value (1 to 2 typically) varying with the width of the drop size distribution.

In general, drop sizes vary considerably with fog type, liquid water being a more conservative property, particularly near the surface. Therefore, drop-size distribution shifts offer considerable latitude for visibility improvement. For example, the fog models developed on this program showed that coastal fogs possess on the average three times greater visibilities than inland fogs, primarily because of their respective drop-size distribution characteristics (despite the fact that coastal fogs have somewhat higher water content). Hence, since the inception of this program, modification concepts have been stressed that showed promise of altering drop-size distributions.[1] Concepts that also incorporate the potential for decreasing fog-water content are, perhaps, most advantageous. While a preferred goal might be complete elimination of fog hydrometeors, historically the payload requirements to accomplish this have proven prohibitive.

As stated, hygroscopic particles introduced into fog can lower the relative humidity and cause evaporation of natural fog droplets. Limited success of this concept has been due, in part, to an inability to disperse hygroscopic particles of the proper size into the atmosphere. Obviously, if submicron particles are used for seeding, the resultant drops will be undesirably small, possibly leading to increased scattered light and even poorer visibility. On the other hand, if excessively large particles are introduced into the fog, total mass requirements render the scheme inefficient. Some of the key questions then that had to be answered to evaluate the concept were:

1. What are the rates of growth of giant hygroscopic nuclei and the fall times through given depths of fog?

[1] For example, the earlier droplet monolayer work, surfactant-coalescence effort, and droplet electrification analysis.

2. What are the optimum sizes of dry salt nuclei in terms of dwell time in the fog and mass seeding requirements?

3. If only fractional ($\leq 1\%$) reductions in relative humidity are obtained, will significant evaporation of the natural fog drops occur to improve visibility?

1. Droplet Growth versus Fall Distance (time)

We wish to derive an expression for the size achieved by giant hygroscopic particles after falling through a given depth of fog and the fall time involved. Essentially, this involves combining three equations: a form of the equation for droplet growth by diffusion, the terminal velocity equation, and Stokes expression for the terminal velocity of spheres. The droplet growth equation employed is that given by Fletcher (1962):

$$r \frac{dr}{dt} = G\left(S - \frac{a}{r} + \frac{b}{r^3}\right). \tag{2}$$

Equation symbols are defined in Appendix C. The right hand side of the equation is seen to express the four well-known growth factors: heating (G), environmental supersaturation (S), Kelvin curvature effect (a/r), and nucleus solubility (b/r^3).

For giant nuclei, $a/r \ll b/r^3$, and assuming only slight humidity changes, S = O (i.e. relative humidity R. H. = 100%). With these simplifications, equation (2) reduces to

$$dt = r^4 \, dr / Gb. \tag{3}$$

Stokes equation.

$$v = \frac{2}{9} r^2 g \frac{(\rho_o - \rho_a)}{\eta} \simeq \frac{2}{9} \frac{\rho_o g r^2}{\eta} \tag{4}$$

Velocity equation. $$dh = v\,dt \tag{5}$$

Substituting equations (3) and (4) into (5) and integrating yields the fall distance H and size r_H achieved by droplets condensing on nuclei of characteristic b:

$$H = \frac{2}{63}\,\frac{\rho_o g}{\eta G b}\left(r_H^7 - r_o^7\right) \quad and \tag{6}$$

$$b = 4.3\,i\,\frac{m_s}{M} \tag{7}$$

where salt nucleus mass and molecular weight are given by m_S and M, and i is the Van't Hoff dissociation factor. For sodium chloride particles, b $\simeq 0.147 m_S$, and equation (6) becomes

$$H = 0.216\,\frac{\rho_o g}{\eta G m_s}\left(r_H^7 - r_o^7\right) \tag{8}$$

2. Numerical Estimates of Droplet Growth and Seeding Requirements

Fog seeding experiments were conducted in a 600 m^3 test facility at Ashford, New York, which is described in section III-B. In preparation for the experiments, calculations were made using the prior expressions. The model fog and seeding conditions assumed were as follows:

(a) Fog depth H = 10 m (height of facility)
(b) Temperature 20°C; Saturation vapor density 18 g m^{-3}
(c) Fog drop radii 5μ
(d) Fog liquid water content 0.2 g m^{-3}
(e) Salt (NaCl) injected at top of fog
(f) Saline droplet density ρ_o = 1.1 cm^{-3}
(g) Initial salt particle radius $r_o \ll r_H$ and can be ignored.

Invoking the above conditions, equation (8) can be solved for droplet size r_H achieved after a fall of 10 m as a function of salt nucleus mass. Particle dwell time in the fog is obtained by integrating equation (3). Thus, the approximate relations for final droplet size and time of fall of particles in the Ashford fog facility are as follows:

$$r_H = 515\ m_s^{1/7} \tag{9a}$$

$$t_H = 1.11 \times 10^{-14}\ r_H^{5}/m_s \tag{9b}$$

where the units are r_H in microns, H in cm, and m_s in g. The mass m_p of water absorbed by each hygroscopic particle is

$$m_p = \rho_o \tfrac{4}{3} \pi r_H^3 - m_s \tag{10}$$

Using equation set (9a and b), the final drop size and fall time of droplets in the chamber were calculated as a function of salt nucleus size. The mass of water extracted from the fog per giant nucleus was determined (equation 10), as well as the total concentration and mass of salt needed to fulfill the indicated clearing objective, i.e. to absorb 0.2 g m^{-3} of fog water. The resulting estimates are shown in Table I.

Note that the figures in Table I relate to a constant relative humidity of 100 percent. This degree of seeding may be thought of as that just sufficient to evaporate the natural fog droplets and to transfer the vapor to the absorbing salt particles. (Droplet evaporation rates are considered in the next section.) Thus an initial visibility improvement is to be expected from an upward shift in the drop size distribution; subsequently the larger saline drops commence to fall out of the system thereby decreasing liquid water and improving visibility further.

Table I

DROPLET GROWTH AND FOG SEEDING REQUIREMENT - 100% R.H.

(MODEL FOG CONDITIONS: T = 20C, FOG DEPTH = 10m, FOG LWC = 0.2 g m^{-3}, DROP RADII = 5μ, WATER ABSORBED BY SALT = 0.2 g m^{-3})

SALT PARTICLE RADIUS (MASS)	FINAL DROP SIZE r_H	FALL TIME t_H	WATER PER PARTICLE m_p	REQUIRED SALT CONC.	REQUIRED SALT MASS ($600m^3$)	VISIBILITY IMPROVEMENT FACTOR
47.8μ (10^{-6}g)	71.5 μ	21 sec	54.0×10^{-8}g	0.37 cm^{-3}	220g	14
22.4 (10^{-7})	51.5	40	47.4	0.42	25	10
10.0 (10^{-8})	36.8	76	19.9	1.0	6.0	7
4.78 (10^{-9})	26.3	141	7.60	2.6	1.6	5
2.24 (10^{-10})	18.9	270	2.84	7.0	0.42	3.5
1.0 (10^{-11})	13.7	536	1.08	18.5	0.11	2.5
0.48 (10^{-12})	10.0	1110	0.42	47.6	0.024	2

An idealized estimate of maximum visibility improvement that can be obtained solely by shifting the drop-size distribution is shown in the last column of Table I. These values result from application of the Trabert visibility formula (equation 1) and the simplifying assumption of monodisperse drop sizes, i.e. the initial model fog radii of 5μ convert to the final sizes shown in column 2 after appropriate seeding. Since total liquid water is quasi-constant, the visibility improvement factor is merely the final drop radius divided by the initial fog-drop radius (5μ). For example, 2.2μ radius salt nuclei introduced into the fog in concentrations of 7 cm^{-3} (0.42 g total) should grow to 18.9μ radius droplets during their residence time. This corresponds to a visibility improvement factor of about 3.5. After 270 seconds, the drops then settle out and further improvement in visibility is to be expected. (This trend of events is confirmed by the experiments described in section III-B.)

If more salt particles are used in order to reduce the ambient relative humidity and to speed evaporation, saline-drop growth rates will decrease and particle dwell time increase. Equation (3) then takes the form

$$r \frac{dr}{dt} = G(S + b/r^3) \tag{11}$$

To obtain a bound on the salt requirement under these more involved conditions, we considered the equilibrium situation where S had attained an assumed value of -1% (RH = 99%) and -4% (RH = 96%). Integrating equation (11) leads to:

$$t = \frac{r^2}{5G}\left[(S + br^{-3})^{-1} + \frac{3}{8} S(S+br^{-3})^{-2} + \frac{9}{44} S^2(S+br^{-3})^{-3} + \frac{81}{616} S^3(S+br^{-3})^{-4} + \cdots\right] \tag{12}$$

The data in Table II were compiled by applying this equation for the largest salt particles, a more rigorous numerical solution for the smaller salt particles (Jiusto, 1967) and approximating the average fall velocity of the growing droplets. We may think of the salt seeding assumed for generating these data as that required to absorb the liquid water in the fog (0.2 g m^{-3}) and to dry the environment by 1% R.H. (approximately 0.2 g m^{-3}).

Note that slight temperature effects due to the heat of solution of the NaCl, heat of condensation of water vapor on the salt nuclei, and cooling via evaporation of natural fog drops were ignored. Owing to the small mass of salt and the slight humidity reductions involved, these modest temperature variations are of secondary importance.

The following conclusions can be drawn based on an analysis of the data presented in Tables I and II:

Table I - 100% RH

1. As salt particle size decreases, the total payload required to absorb 0.2 g m^{-3} of fog liquid water steadily decreases. Particle fall time in the 10 m high fog undergoes a corresponding increase, reaching prohibitively large times for salt nuclei less than about 1μ radius.

2. The larger salt nuclei lead to bigger (fewer) drops and better visibilities. Initially, when liquid water content is essentially constant, the visibility improvement is directly proportional to the final drop size achieved. However, the choice of larger particle size is not unlimited as payloads go up accordingly.

3. The optimum salt particle radius, considering final drop size, fall time, and total required mass, is approximately 5μ. Particles from 2 to 10μ radius appear suitable.

4. Our milled salt consisted of particles of which 85 to 90 percent by number were between 1 and 5μ radius. Table I would predict initial visibility improvements of about 2 to 5, consistent with most of our laboratory observations.

Table II

DROPLET GROWTH AND FOG SEEDING REQUIREMENT - 99% RH
(96% VALUES IN PARENTHESES)

(MODEL FOG CONDITIONS: SAME AS TABLE 9
EXCEPT WATER ABSORBED BY SALT = 0.4 g m^{-3})

SALT PARTICLE RADIUS (MASS)	FINAL DROP SIZE r_H	FALL TIME t_H	WATER PER PARTICLE m_p	REQUIRED SALT CONC.	REQUIRED SALT MASS (600 m^3)
47.8μ(10^{-6}g)	60μ	25 sec	44.5x10^{-8}g	0.9cm^{-3}	540 g
22.4 (10^{-7})	45	50	31.9	1.3	75
10.0 (10^{-8})	30 (20)‡	100 (200)	11.4	3.6	21 (210)
4.78(10^{-9})	22 (12E)	200 (600)	4.80	8.0	5 (60)
2.24(10^{-10})	11E*(6E)	800 (3000)	0.604	66	4 (45)
1.0 (10^{-11})	5E	3000	0.0565	710	4
0.48(10^{-12})	2.4$_E$	14000	0.00629	6400	4

*E INDICATES THAT THE EQUILIBRIUM SIZE OF THE SALINE DROPLET HAS BEEN REACHED

‡ ( ) GIVE VALUES CORRESPONDING TO AN AMBIENT DECREASE IN R.H. TO APPROXIMATELY 96%

5. While more salt is required, somewhat larger particles are desired to enhance droplet sizes and fall times and to take advantage of more rapid visibility improvements through decreasing liquid water content.

Table II - 99% RH

1. Slight (1%) lowering of the ambient relative humidity speeds the evaporation of natural fog droplets, but increases the salt requirement of 5μ radius and larger particles by about a factor of 3 (factor of about 30 for 96% RH objective).

2. Particles 2μ radius and smaller are now entirely undesirable as they soon achieve equilibrium sizes that are ineffectively small. (At 96% RH, 5μ radius nuclei are of limited use.)

3. Optimum particles sizes are about 5 to 10μ radius, with less tolerance for departures from this range than in the previous saturated case.

4. Thus "excessive" drying of the environment, while facilitating natural fog droplet evaporation, can stabilize the growth rate of injected giant nuclei and partially impede desired improvements in visibility. This is not critical if appropriately large nuclei are used that fall out of the system in reasonable times.

The foregoing analysis suggests that effective fog clearance with hygroscopic nuclei entails many considerations and compromises between required payloads, drop sizes, and fall times of particles. A comparison of Tables I and II shows that it may be desirable to seed with just enough material to promote complete evaporation of natural fog droplets and leave the ambient atmosphere near saturation after the evaporation is complete. A priori information on fog depth, liquid under content, and wind speed must be considered in advance of an operation. The ability to specify and generate salt nuclei of desired sizes is essential. These factors were considered in the controlled Ashford fog tests, and as is shown in section III-B, theory and observation were in good agreement. Whether the free atmosphere, with its added variables, is as accommodating remains to be determined.

3. Evaporation Rate of Droplets

As noted previously, sufficient water vapor must be extracted from the fog air by the giant salt nuclei to allow the natural fog droplets to evaporate. The rate of evaporation is, of course, dependent on ambient relative humidity. At the slight subsaturations involved (or at RH = 100%), will evaporation rates be significant?

Numerical calculations of evaporation rate as a function of ambient relative humidity were made using equation (2). It was assumed that the natural fog drops had condensed on typical 0.1μ radius nuclei of NaCl. The time required for given size droplets to evaporate, i.e. reach small equilibrium sizes, was determined and the results plotted in Figure1.

The speed with which small droplets (typical inland fog size shown) evaporate is both revealing and encouraging in terms of the fog seeding objective. Our model fog droplets of 5μ radius will evaporate in 10 seconds at 99% RH, 1.3 minutes at 99.9% RH, and 6 minutes at 100% RH.

Thus, excessive drying of the atmosphere, which was shown in the last section to lead to prohibitively large salt masses, does not appear essential. An optimum ambient humidity to strive for, recognizing that such control is not generally possible in practice, is approximately 99.5 to 99.9 percent RH.

4. Hypothetical Airport Clearing

The foregoing analysis was extended to obtain an estimate of the requirements and feasibility of clearing a hypothetical airport fog. The fog volume considered was 10^8 m^3, equivalent to a zone 500 m wide, 100 m high, and 2000 m long. Model fog conditions, except for height (now 100 m high), were as stipulated in Table I: 0.2 g m^{-3} LWC; 5μ radius drops; 20°C Temp; 100% RH seeding objective.

The seeding effects and requirements are indicated in Table III. Again, 5μ-radius salt nuclei appear optimum. As such, 90 kg of material is required for one seeding, in which case an initial (idealized) visibility-improve-

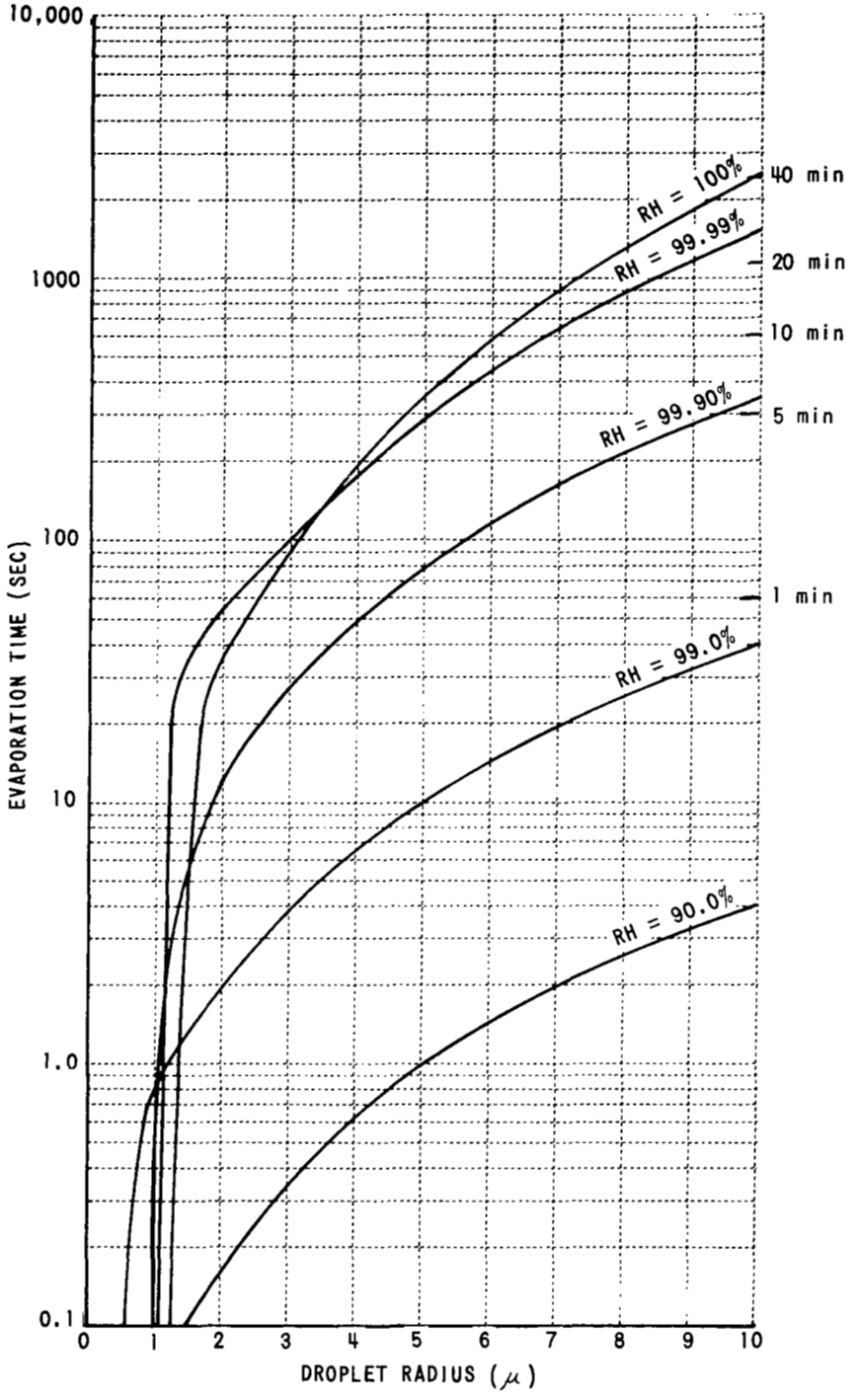

Figure 1 EVAPORATION TIMES OF DROPLET vs RELATIVE HUMIDITY
(ASSUMED DROPLET NUCLEI - 0.1 RADIUS NaCl PARTICLES)

Table III

HYPOTHETICAL FOG CLEARANCE AT AN AIRPORT

MODEL FOG: FOG HEIGHT AT 100 m, 0.2 gm^{-3} LWC,

5 μ RADIUS DROPS, T = 20 C ; RH = 100%

SALT PARTICLE RADIUS (MASS)	FINAL DROP SIZE	FALL TIME t_H	WATER PER PARTICLE MP m_p	REQUIRED SALT CONC.	REQUIRED SALT MASS (10^8 m^3)
47.8 (10^{-6}g)	99.3μ	110 SEC	206. x 10^{-8}g	0.098 cm^{-3}	9720 kg
22.4 (10^{-7})	71.6	210	179.	0.112	1120
10.0 (10^{-8})	51.1	390	61.5	0.325	325
4.78 (10^{-9})	36.5	730	22.2	0.901	90
2.24 (10^{-10})	26.3	1400	8.36	2.39	24
1.0 (10^{-11})	19.04	2780	3.17	6.31	6.3
0.48 (10^{-12})	13.9	5760	0.887	22.6	2.3

ment factor upwards of 7 might be achieved. With a 3 m/sec wind velocity, about 5 such seedings per hour or 450 kg/hr would be required for continuous airport operation. Should faster particle fall times prove necessary, the use of say 10μ radius nuclei would dictate corresponding seeding rates of 1600 kg/hr. The concept might then be testing the limit of feasibility. (It is of interest to note that on a comparable volume basis, this requirement is still over 2 orders of magnitude lower than that required by Houghton and Radford to decrease fog humidity to 90%.)

It should be emphasized that the foregoing values are first-order estimates subject to further refinement and field verification. Complicating factors such as particle size variations, inhomogeneities in atmospheric salt distribution (particles will be blown up from ground level rather than released at fog top), heating and cooling effects, and turbulent diffusion will all influence the contemplated field experiments. Nevertheless, a reasonable understanding of the processes involved in the laboratory situation has been obtained such that the next logical step - field experimentation - is warranted.

B. Fog Seeding Experiments in the 600 m^3 Chamber

1. Equipment

Fogs were produced in the CAL Ordnance Laboratory located at Ashford, New York. The facility, pictured in Figure 2, consists of a cylindrical chamber which can be pressurized or evacuated at controlled rates. In essence, adiabatic expansions are produced, and under appropriate humidity conditions, fogs form. These laboratory fogs were found to possess liquid water contents and drop-size distributions that are representative of natural inland fogs.

The large chamber is 30 ft in diameter and 30 ft high, enclosing a volume of approximately 600 m^3. Construction material consists of 0.5 inch sheet steel with an epoxied inner surface. As shown, a rotating spray nozzle enables the walls and floor of the chamber to be thoroughly wetted with water, and the relative humidity of the air to approach 100%. Glass ports are located at various levels for monitoring the fog visually or with transmissometers. Ports in the domed ceiling allow convenient dispersal of seeding material.

By means of a blower-circulation system, the chamber can be pressurized to approximately 20 cm of water. After permitting the internal temperature and humidity to equilibrate with the wet walls, the chamber can then be vented to the outside at controlled rates. Adiabatic expansions are thereby produced. Alternately, air can be vacuum-pumped out of the large chamber at controlled rates to produce the expansion. With either operating method, representative fogs can be formed for subsequent seeding experiments.

The fogs formed in the above manner slowly decay as the droplets evaporate. Typical working times are approximately 20 to 25 minutes. It was found that more persistent fogs could be generated by initiating a slow secondary expansion following the initial fog-forming expansion. Moreover, fog visibility essentially could be held constant by appropriately controlling the secondary expansion.

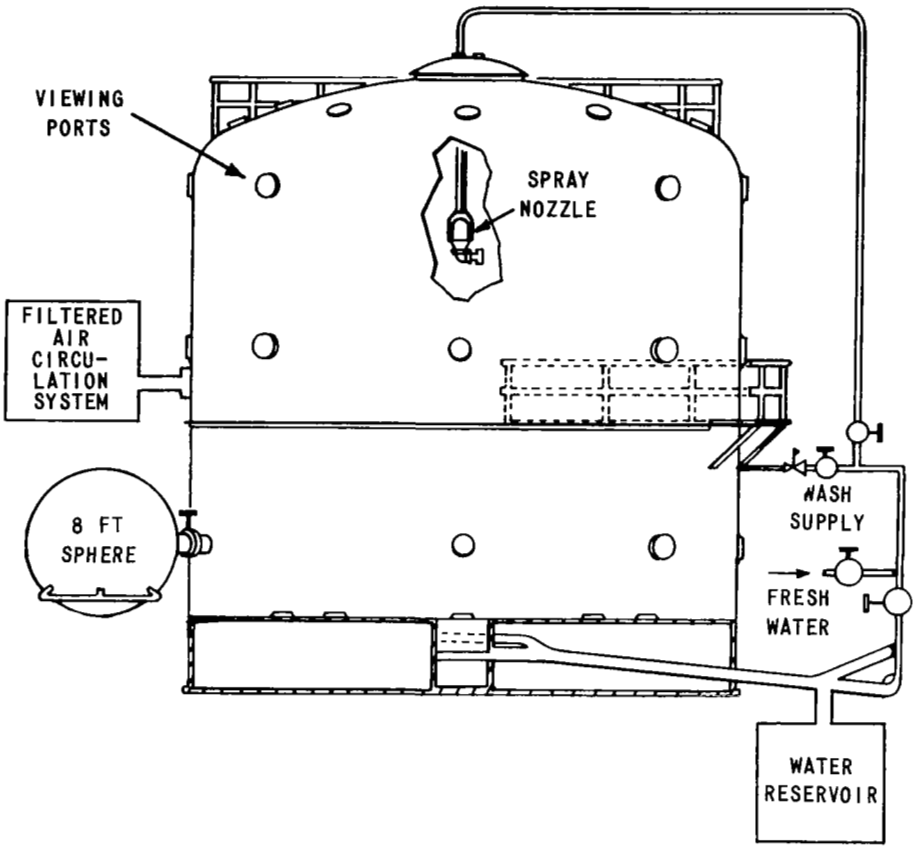

Figure 2 THE 600m^3 TEST CHAMBER AT ASHFORD, NEW YORK

The primary sensors used to monitor fog characteristics are outlined below:

1. Two transmissometers for recording horizontal visibility (i.e. extinction coefficient) over a 60 ft path (30' baseline with reflecting mirror). One transmissometer was located at a 4 ft high level, the second at 15 ft.

2. A fog-droplet sampler, employing a gelatin replication technique, for measuring drop-size distributions during the fog's life cycle.

3. Psychrometric equipment for estimating relative humidity (at the lower level only).

4. Temperature sensors arrayed vertically at heights between 4 and 24 ft.

5. Cloud nucleus counter and Aitken counter for monitoring condensation nucleus concentrations.

Transmissometer data and temperature information were recorded

externally, while the other equipment was manually operated from within the chamber. Visual observation, by the operator, of fog characteristics and seeding plumes added substantially to the experiments.

The artificial nuclei were injected into the chamber through a small port (located 8 ft from the center line) in the chamber dome. The particle classifier-disseminator described in Appendix A was used for seeding the fogs. The size distribution of the sodium chloride particles produced by this equipment, is shown in Figure 3.

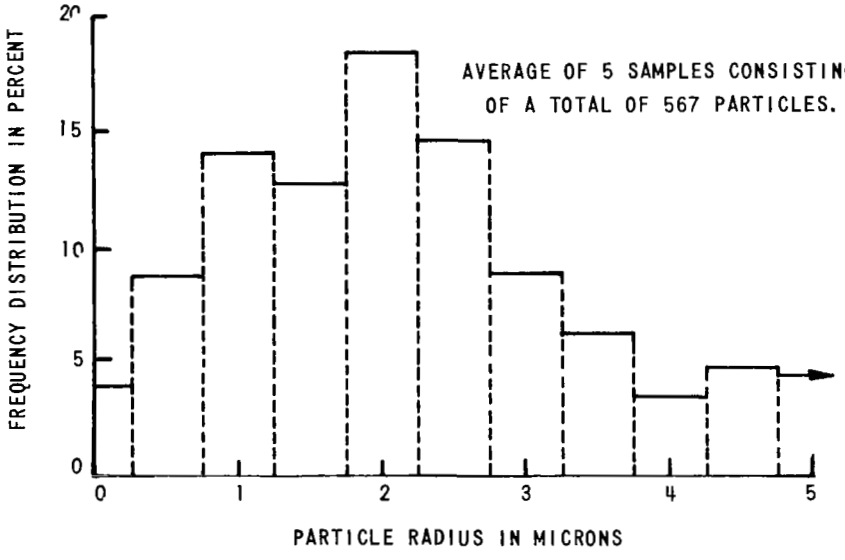

Figure 3 SIZE DISTRIBUTION OF NaCl NUCLEI PRODUCED BY THE PARTICLE CLASSIFIER-DISSEMINATOR USED IN THE FOG SEEDING EXPERIMENTS

2. Summary of Visibility Improvements Achieved in Laboratory Seeding Experiments

The primary objectives of fog seeding experiments at Ashford, N. Y. were: 1) to determine the maximum improvement in visibility that could be achieved by seeding with NaCl nuclei of carefully controlled size and 2) to determine the minimum amount of material required to achieve the desired visibility improvement. Results of these experiments have demonstrated that visibility in laboratory warm fog can be improved by a factor of at least three and as much as ten by seeding with properly-sized salt particles. Significant improvement in visibility was achieved with as little as 1.7 milligrams of salt per m^3 of foggy air, but no improvement was observed with 0.8 milligrams per m^3. These values are in excellent agreement with the theoretical prediction of 2 mg per m^3 for the nucleus size distributions used in the experiments.

Two types of fogs were involved - those which were slowly dissipating and those of a persistent nature (i.e. fogs showing no improvement in visibility over approximately a 25 minute period). Again, the goal in each of these experiments was to modify the drop-size distribution in such a way as to reduce the Mie scattering coefficient, and thereby improve visibility. Increased precipitation rates that accompanied the drop-size distribution were expected to further improve visibility.

Typical physical characteristics of the laboratory fogs approximately one minute after completion of the expansion are compared in Table IV with the radiation fog model developed during the first year of this program. It is apparent that the similarities are quite good.

The procedure used in the experiments in which fog was dissipating was to produce one fog for use as a control and observe its physical characteristics as it dissipated under natural conditions. A second fog was then produced and seeded with a predetermined mass of NaCl. The physical characteristics of the seeded fog were then compared with the control fog.

Table V summarizes the visibility improvement (seeded fog relative to control fog) as a function of time after seeding for experiments with

TABLE IV

Characteristics of Laboratory Fog and Natural Radiation Fog

Fog Parameter	Laboratory Fog	Natural Radiation Fog
average drop radius	4 to 5μ	5μ
typical drop radius range	2-18 to 2-22μ	2-18μ
liquid water content	150 to 200 mg m^{-3}	110 mg m^{-3}
droplet concentration	250 to 500 cm^{-3}	200 cm^{-3}
visibility	200 to 400 ft	300 to 900 ft
vertical depth	10 m	100 to 300 m

Table V

VISIBILITY IMPROVEMENT FACTOR* FOR SEEDING EXPERIMENTS

FOG SEEDING			
TIME FROM START OF SEEDING			
SEEDING MASS	+4 MIN	+8 MIN	+12 MIN
51 mg m^{-3}	(1.5) [0]	(5.7) [1.6]	(3.6) [6.7]
8 mg m^{-3}	(1.8) [5.1]	(5.0) [9.1]	(1.1) [2.9]
4 mg m^{-3}	(1.4) [2.3]	(7.6) [9.4]	(1.8) [1.6]
1.6 mg m^{-3}	(1.2) [1.2]	(1.7) [4.0]	(4.5) [6.7]
.8 mg m^{-3}	(-) [0]	(0) [-1.1]	(0) [-1.1]
51 mg m^{-3} (APRIL '67)	(1.6) [0]	(10) [4.9]	(2.4) [3.9]

( ) INDICATE DATA FROM 15 FT LEVEL
[ ] INDICATE DATA FROM 4 FT LEVEL

*IMPROVEMENT FACTOR IS DEFINED AS THE RATIO OF THE VISIBILITY OF THE SEEDED FOG TO THE VISIBILITY OF THE CONTROL FOG AT THE SAME TIME AFTER INITIATION OF THE EXPANSION

dissipating fog. Results of the experiments on persistent fog are shown in Figure 4. The solid and dashed curves show fog visibility as a function of time for control and seeded fogs respectively. Eight mg of NaCl per m^3 were injected into the fog top in this experiment. It is noteworthy that even though the secondary expansion caused extreme additional cooling

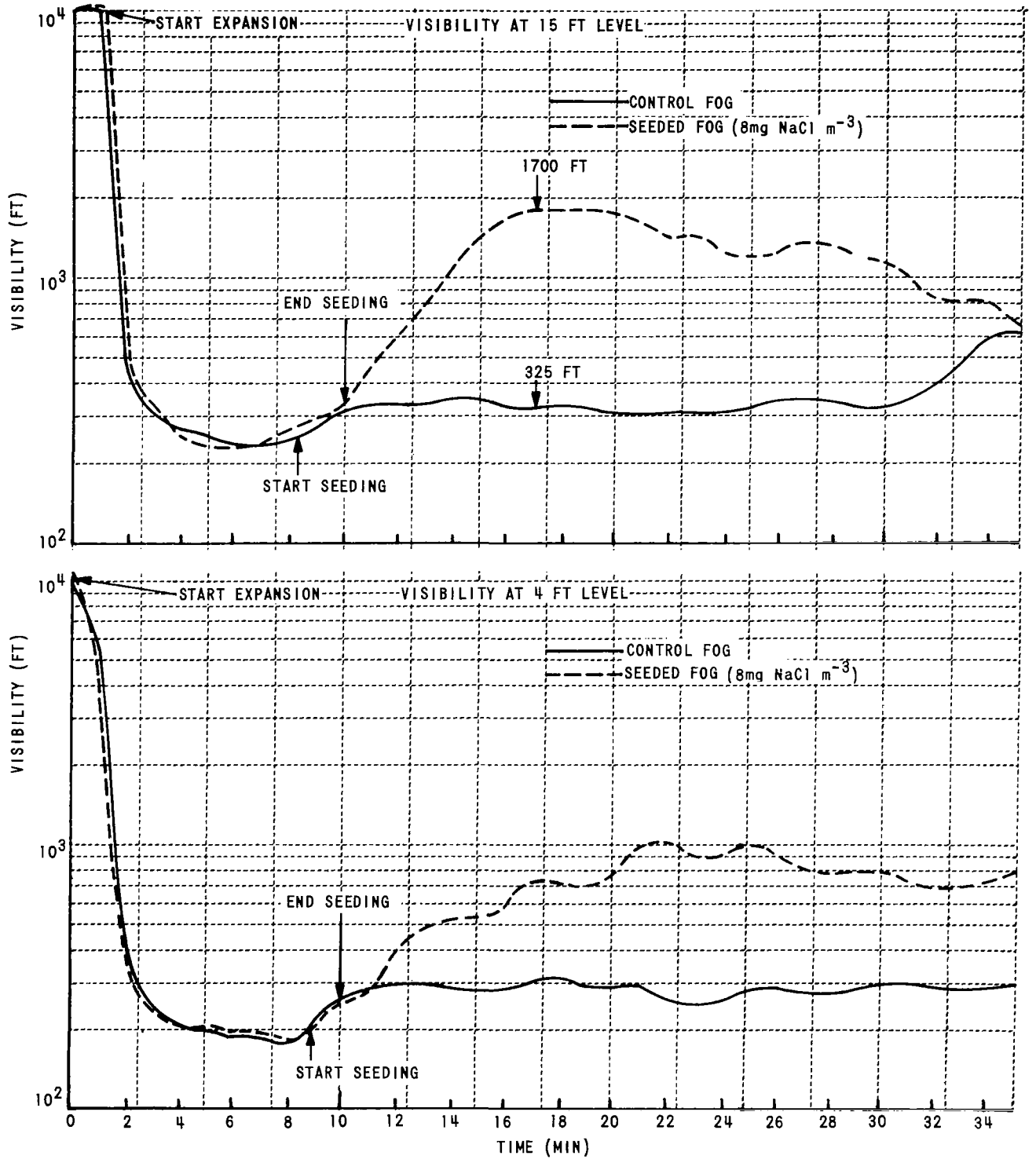

Figure 4 VISIBILITY AS A FUNCTION OF TIME FOR A SEEDED AND CONTROL FOG

at a rate of four degrees per hour, visibility was improved by a factor of more than five at the upper transmissometer level and more than three near the fog base.

3. Analysis of the Processes Responsible for Visibility Improvements

The fact that the seeding procedures used in these experiments produced significant improvements in visibility is established by the transmissometer data. Two participating mechanisms are the change in drop-size distribution and the decrease in liquid water content (LWC) caused by precipitation of large drops. This analysis is aimed at determining the relative contributions of the two mechanisms to the visibility improvement.

Measurements of the size distribution of droplet samples collected on gelatin-coated slides show that a modification of the distribution was accomplished. With our droplet-sampling apparatus, uncertainties in the exposure time of coated slides in the air stream prevented direct measurement of absolute droplet concentration, although size distribution data were obtained. To obtain droplet concentration and hence permit calculation of LWC, drop-size distribution information can be combined with transmissometer data in the following manner.

The intensity of light observed with a transmissometer is given by

$$I = I_o \; e^{-\beta x} \tag{13}$$

where I_o is the intensity observed in clear air, β is the extinction coefficient and x is the length of the transmission path in the fog.* Visibility is computed from such data according to

$$V = \frac{K}{\beta} \tag{14}$$

where K is a constant.

*The extinction coefficient consists of the absorption coefficient, the Rayleigh scattering coefficient and the Mie scattering coefficient. In fog only the Mie scattering coefficient is important.

β is related to the drop size distribution, $N(r)$ according to

$$\beta = E\int_o^\infty N_i(r)r^2dr \tag{15}$$

where the subscript i designates the particular fog being sampled and E is the scattering efficiency factor. For droplets of diameter greater than approximately one micron E is equal to 2π.

From the drop-sample data, we are able to compute

$$\frac{\beta_i}{N_i} = \frac{E\int_o^\infty N_i(r)r^2dr}{\int_o^\infty N_i(r)dr} \tag{16}$$

which is the average scattering cross section (extinction coefficient) per droplet. N_i is the number of droplets per unit volume (to be determined). Since β is determined independently from equation (13) using transmissometer data, N_i can be computed from:

$$N_i = \beta_{TRANS} \Big/ \left(\frac{\beta_i}{N_i}\right) \tag{17}$$

where the quantity in the denominator is given by equation (16).

The liquid water content of the fog is given by

$$W_i = 4/3\,\pi\rho\int_o^\infty N_i(r)r^3dr \tag{18}$$

where ρ is the density of liquid water. Again, from the drop sample data we can determine only

$$\frac{W_i}{N_i} = 4/3\,\pi\rho\,\frac{\int_o^\infty N_i(r)r^3dr}{\int_o^\infty N_i(r)dr} \tag{19}$$

Substituting the value of N_i determined from equation (17) into equation (19) provides the estimate of liquid water content.

4. Accuracy of Measurements

The basic transmissometer signal is measureable to about 1% accuracy. When operated with the mirror in the chamber, condensation and splashing of drops falling off of the chamber walls and impacting near the mirror limit overall certainty in determination of I and I_o to approximately 10%. This in turn transforms to an uncertainty in β (the scattering coefficient) of about 5%.

The accuracies of drop-size distributions are limited primarily by the relatively small number of droplets counted. Our samples usually consisted of between 200 and 300 droplets. Thus, with many of the drop-size distributions in the seeding experiments, only fifteen to thirty of the very large droplets (i.e. larger than those found in the corresponding control fog) were counted. A 20 to 25% uncertainty in the concentrations of these large particles can therefore be expected as an average for a large number of experiments. Errors of 50% are not unlikely for individual experiments. Since these large particles contribute most, both to the Mie scattering coefficient and liquid water content, estimates of both of these quantities are expected to contain random errors of at least 25% and perhaps in some cases as much as 50%. The analyses described are consistent with this degree of accuracy and should not be given more precise interpretation.

5. Results Obtained from Seeding Fogs

Figure 5 is a typical example of droplet replicas obtained on gelatin-coated slides. Such samples were obtained on specially cut slides, 1.5 mm wide, that were automatically exposed to the fog. (Velocity of the airstream, 32 m/sec, in which collections were made, was measured with a hot wire anemometer.) Previous calibrations have shown that the diameter of the droplet impressions are twice the true drop diameter to within ± 10%.

Droplet measurements were obtained from photomicrographs similar to those shown in the Figure 5. Collection-efficiency corrections were

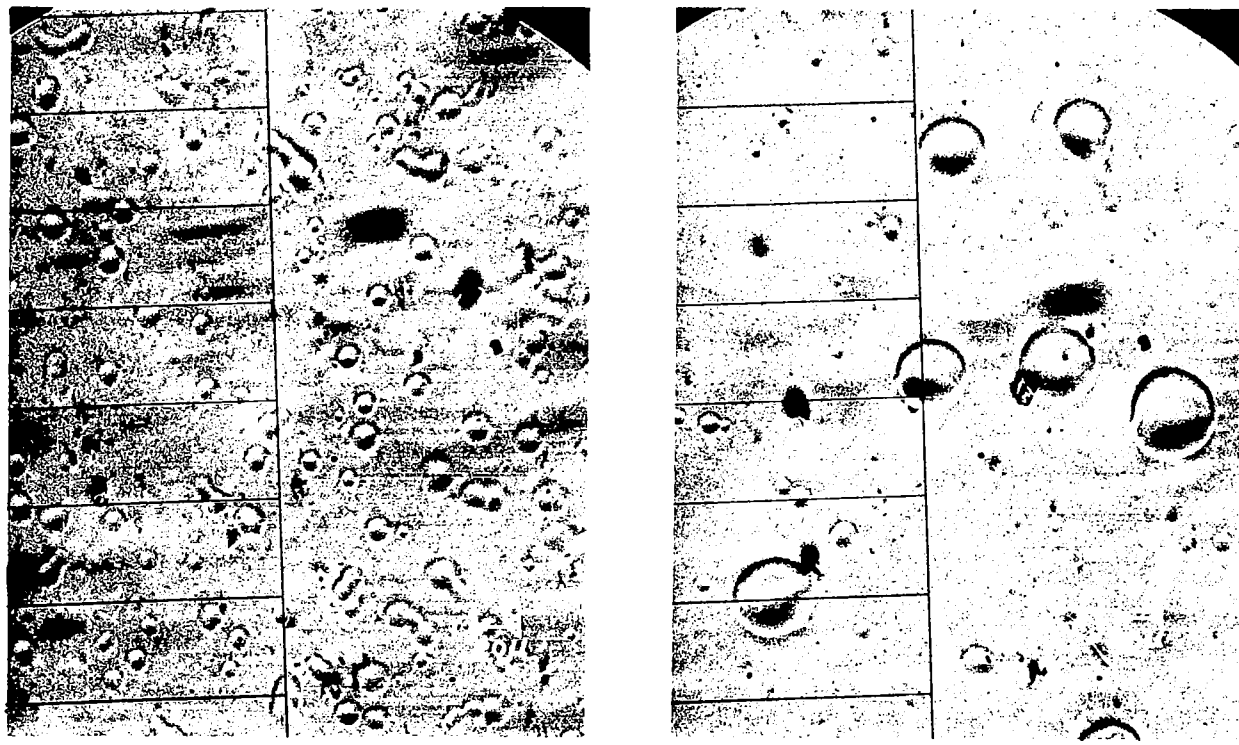

CONTROL FOG

SEEDED FOG

Figure 5 DROPLET IMPRESSIONS OBTAINED AT T = 20 MINUTES IN THE PERSISTENT FOG EXPERIMENT. SCALE SHOWN IS FOR TRUE DROP SIZE.

applied to the raw data and equation (17) was used to determine total droplet concentration. A typical example of the final drop-size distributions obtained is shown in Figure 6.

Figures 7 and 8 depict visibility as a function of time as determined from transmissometer data in representative fog-seeding cases. The (b) portion of each of these figures shows how the changes in liquid water content (determined from the previously-described analysis) would have contributed to the variations in visibility if the drop-size distribution had not changed. Under these conditions visibility is inversely proportional to LWC. The (c) portions of these figures indicate how changes in drop-size distribution would have contributed to visibility variations if liquid water content had been invariant. (The ratio of equation (16) to equation (19) is an estimate of the Mie scattering coefficient per unit volume of water. The quantity plotted is the normalized value of the reciprocal of this ratio.)

Since the visibility variations were due to a combination of the two effects shown, the actual change in visibility depicted by the (a) curves is equal to the product of the variations due to liquid water content and drop-size distribution changes. For example, in the seeded fog shown in Figure 7(a), the visibility at $t = 10$ minutes was 250 feet and at $t = 15$ minutes was 2500 feet - a factor of 10 improvement. From the figure (b and c curves) it can be seen that the change in drop-size distribution caused a visibility improvement factor of 3.2 and the change in LWC caused an additional improvement factor of 3.2, hence accounting for the total visibility improvement. For the control case the entire variation in visibility (a factor of 2) over the same time interval was due to a decrease in liquid water content.

In order to compare seeded and unseeded fogs it is necessary to consider the ratios of the various quantities in question at the indicated time. For example, in Figure 7(a) the improvement in visibility of the seeded fog over the control fog at $t = 15$ minutes is a factor of 5.0. The five-fold improvement can be accounted for by liquid water content differences (a factor of 1.5) and changes in drop-size distribution (a factor of 3.3 improvement). The data presented therefore are useful for studying

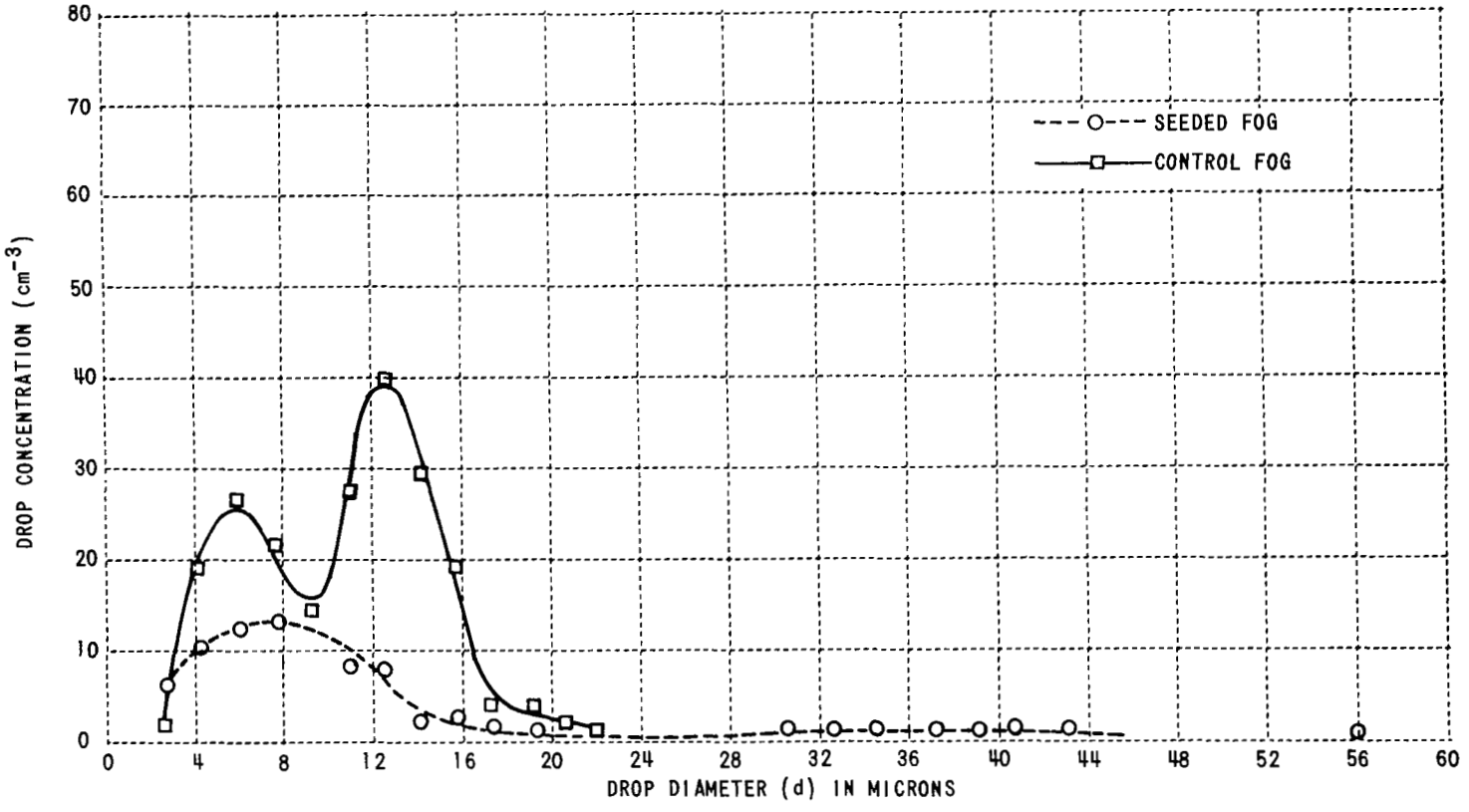

Figure 6 DROP SIZE DISTRIBUTIONS FOR SEEDED AND UNSEEDED FOGS AT T = 20 MINUTES IN THE PERSISTENT FOG EXPERIMENT

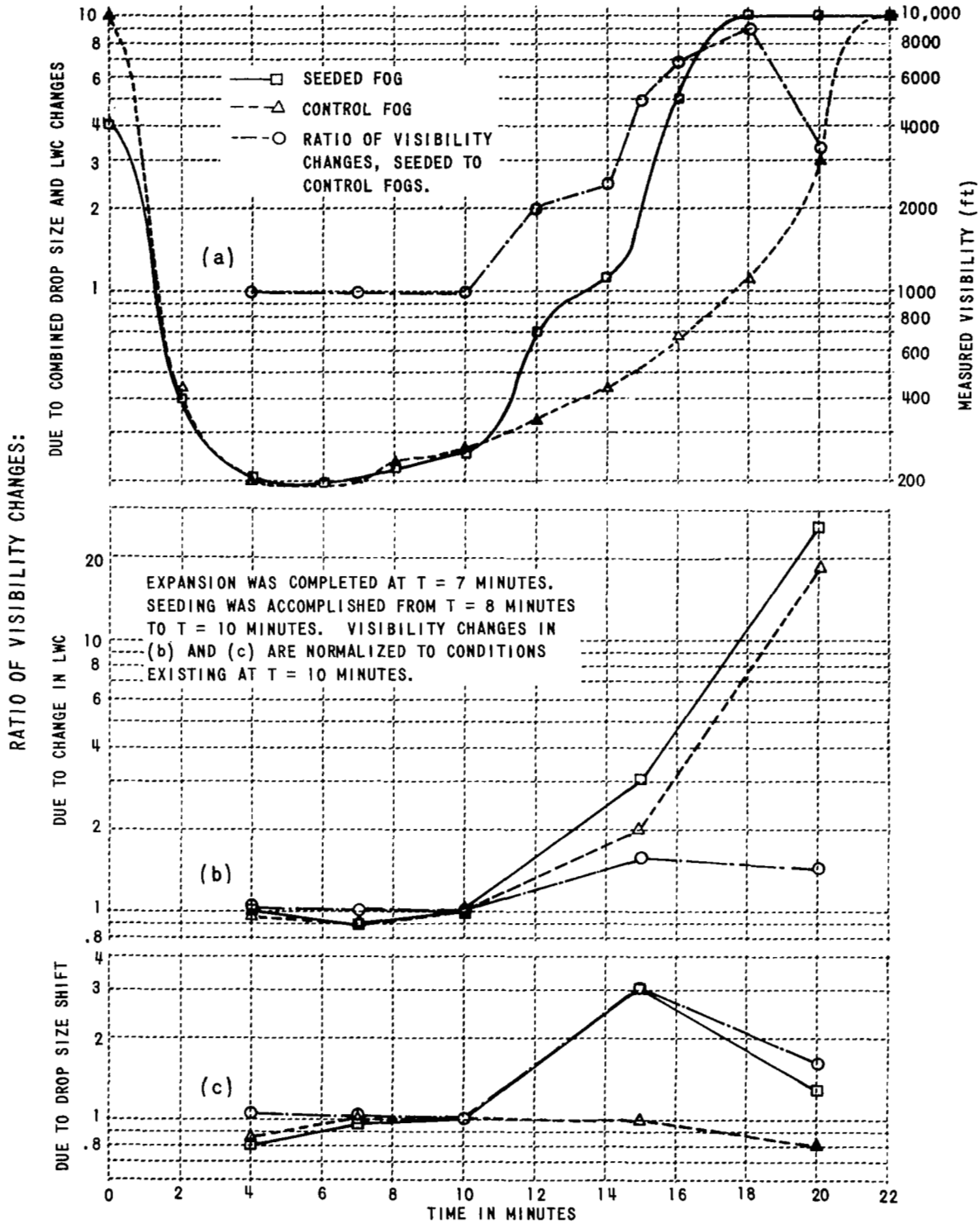

Figure 7 FOG SEEDING RESULTS - DISSIPATING FOG

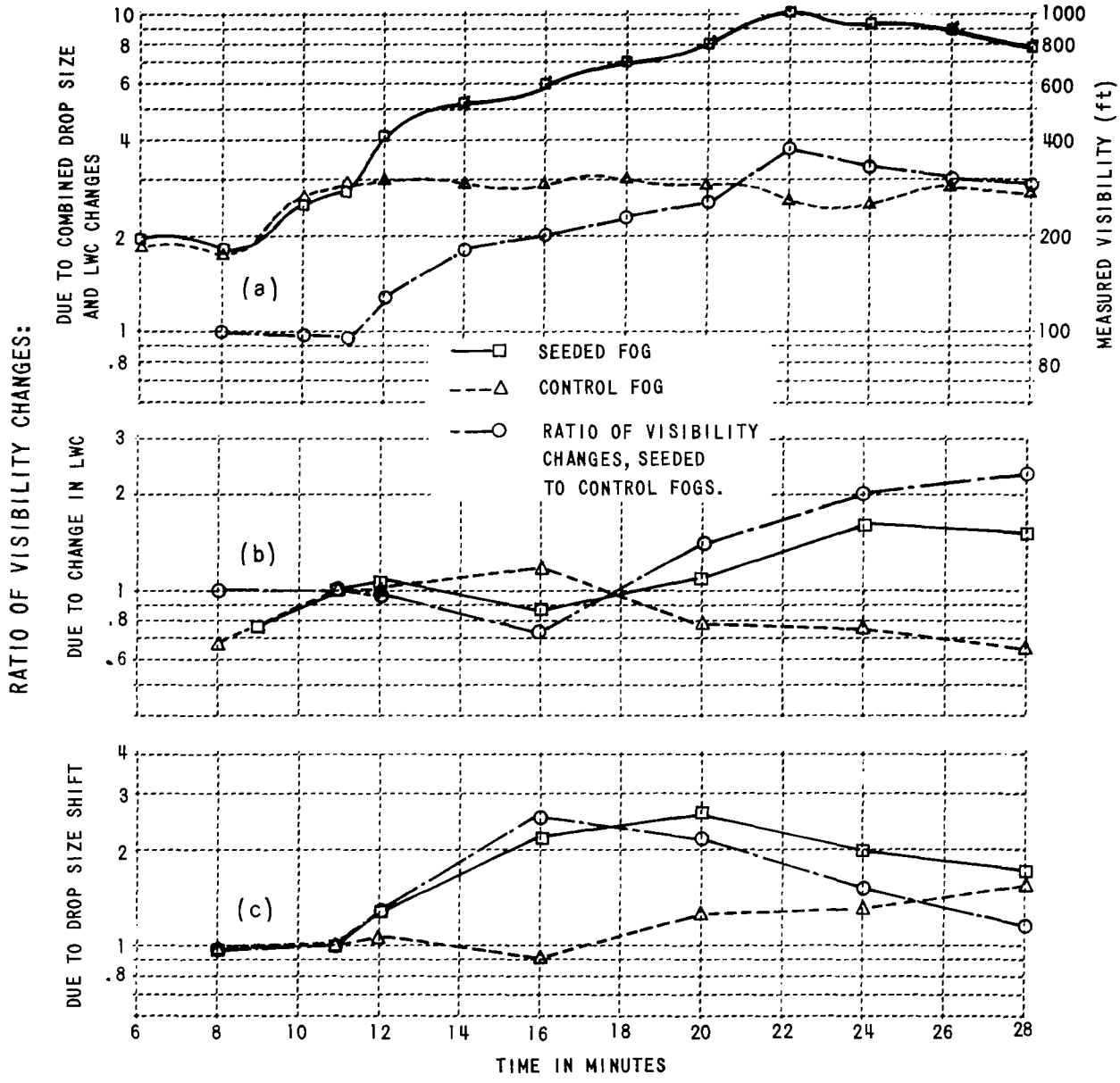

INITIAL EXPANSION WAS COMPLETED AT T = 8 MINUTES. SEEDING WAS ACCOMPLISHED FROM T = 8.5 MINUTES TO T = 10 MINUTES. SECONDARY EXPANSION WAS INITIATED AT T = 11 MINUTES. VISIBILITY IMPROVEMENTS IN (b) AND (c) NORMALIZED TO CONDITIONS EXISTING AT T = 11 MINUTES.

Figure 8 SEEDING RESULTS - PERSISTENT FOG

visibility variations in individual fogs and for comparing seeded fogs to control fogs . By t = 17 minutes the visibility had increased to 10^4 ft, the upper limit of sensitivity of the transmissometer.

The results obtained in Figure 7 pertain to seeding a slowly dissipating fog with 4.0 mg of NaCl m^{-3} of air. The expansion was terminated for both the seeded and control fog at t = 7 minutes. The slow dissipation of the control fog began almost immediately and accelerated throughout the period analyzed. It is evident that this visibility increase was almost entirely due to a decrease in liquid water content (probably caused by evaporation of the droplets as air temperature increased to that of the chamber walls).

In summary, the salt seeding produced an overall improvement in visibility of a factor of five at t = 15 minutes, five minutes after seeding. This improvement is consistant with the results predicted theoretically and shown in Tables I and II.

The data shown in Figure 8 were obtained in fog produced by an initial expansion from an overpressured chamber into the ambient atmosphere. This initial expansion was terminated at t = 8 minutes. To prevent the natural dissipation that ensues, a secondary expansion was initiated at t = 11 minutes. The expansion rate necessary to maintain constant visibility corresponded to a cooling rate of 4^{o} C hr^{-1}.

The transmissometer data and the droplet sample data indicate that the seeded and control fogs at the four-foot level were essentially identical up to t = 11 minutes. (At the 15-foot level, initial effects of the seeding were observed at t = 10 minutes, the time seeding was terminated.) At this time the liquid water content of both fogs was approximately 180 mg m^{-3}. The trend of the data indicates that LWC of the control fog increased from 180 to 280 mg m^{-3} from t = 11 minutes to t = 20 minutes. The apparent increase in LWC is undoubtedly the result of (a) activation and growth of droplets due to the secondary expansion and (b) continued droplet growth of existing fog droplets. Because of a corresponding increase in drop sizes, visibility throughout this period remained essentially constant at 300 ft.

In the seeded fog, it appears that there was initially a slight increase in LWC between t = 11 minutes and t = 16 minutes, followed by a return to the initial value at t = 20 minutes and a continued decrease to about 120 mg m^{-3} at t = 28 minutes. This sequence is consistent with our concept of what should be happening, i.e. water vapor should condense rapidly on the salt particles for the first few minutes after they are introduced, thereby increasing LWC; later, as these particles grow, they begin to fall out and remove water from the fog. This trend suggests that the increased precipitation due to seeding slightly exceeds the rate at which liquid water is made available by the additional expansion.

During the period from t = 11 to t = 20 minutes the visibility of the seeded fog increased by a factor of 2.6 - a factor entirely attributable to the change in drop-size distribution. This value is slightly smaller than the improvement expected from droplet growth at 100% relative humidity. The difference in observed and computed values is undoubtedly associated with the increased water made available by the secondary expansion. It is possible to deduce from the drop-size distribution in Figure 6 that in the seeded fog the artificial nuclei could not entirely accommodate both the additional water being made available by the expansion and the water present in the fog before seeding.

Visibility increased to a value of 950 feet at t = 24, a three-fold improvement over the initial value. Of this, an improvement factor of 2 was associated with the drop-size distribution change and a factor of 1.6 associated with the decrease in LWC. Visibility dropped to approximately 800 ft at t = 28 minutes and remained in this vicinity until the end of the experiment at t = 35 minutes. Analysis of the last droplet sample (obtained at t = 28 minutes) indicates that the net improvement in visibility at that time was due to approximately equal contributions from drop-size distribution and LWC changes.

The processes that caused the improvement of visibility of the seeded fog relative to the control fog changed in a consistent manner during the experiment. During the first 8 to 10 minutes after seeding, the shift in drop-size distributions caused virtually the entire visibility improvement.

From that time on, the difference in liquid water content of the two fogs, due to the precipitation of water condensed on the larger salt nuclei, became increasingly important. By t = 28 minutes (18 minutes after seeding was completed) most of the visibility difference between the two fogs was due to the liquid water content reduction. This, we believed, continued to be the predominant effect until the experiment was terminated.

6. Discussion of Results

It is noteworthy that the physical characteristics (drop-size distribution, liquid water content and visibility) of both the control fogs and the seeded fogs at the time of seeding were characteristic of dense natural radiation fogs. These characteristics changed rapidly, however, even in the control fogs. In one type of experiment, rapid natural drying was causing the fog to dissipate; in the other, abnormally high cooling rates, intentionally produced to maintain constant visibility, were causing a rapid increase in liquid water content. Because the two conditions produced in the laboratory straddle most environmental conditions, some inferences relative to the effects of seeding natural fog may be drawn. Since the visibility improvement in the first five minutes due to drop-size distribution changes was a factor of 3 for the dissipating fog and 2.6 for the persistent fog, we believe that in natural fog the initial rate of visibility improvement will be near these values.

The visibility improvements observed at later times in the experiment were strongly influenced by increased precipitation rates. While increased precipitation will occur in a natural seeded fog, the effect cannot become dominant (for the same-size salt particles) as soon after seeding as was observed in the shallow laboratory fogs. Comparison of corresponding values of t_h in Table I (for 10 meters) and Table III (for 100 meters) shows that the time required for precipitation of droplets formed at 100 meters is roughly five times that required for precipitation from 10 meters. The same tables also show that continued growth of solution droplets formed on the artificial nuclei causes a continued improvement in visibility due to drop-size distribution changes that occur after the droplets fall 10 meters.

The potential for this continued improvement is also evident in the experimental data obtained in the persistent fog.

It is obvious from the drop-size distribution shown in Figure 6 that all natural droplets had not evaporated during the first five minutes after seeding. Calculations based on these data show that about 60% of the extinction coefficient at that time was due to droplets having radii characteristic of the control fog. Assuming for simplicity that no additional water is made available 5 minutes after seeding, the equilibrium vapor pressure over solution droplets formed on the salt nuclei is equivalent to approximately 99.3% relative humidity. These droplets would continue to grow and cause evaporation of nonsaline droplets in a thicker fog. If the water contained in the existing nonsaline droplets is redistributed on the solution droplets, it can be shown that the resultant visibility would be about a factor of 2 better than that measured in the shallow (10 m) laboratory fog. Thus, recognizing the differences between the conditions of the experiment and those of the calculations (Section III-A) reasonable agreement between theory and observations is evident.

7. Extrapolation of these Results to Fog Dissipation at an Airport

The conclusion drawn from this investigation is that fog seeding procedures suggested here, in which carefully controlled sizes of NaCl nuclei are used, should produce significant improvements in the visibility of fog at airports. Two processes will effect this change. The initial improvement in visibility will result from a change in drop-size distribution from one consisting of a large concentration of small droplets to one consisting of a smaller concentration of large drops. This change in distribution will be accompanied by a decrease in extinction coefficient, at first without significantly altering the liquid water content. As time progresses precipitation of droplets will result in additional improvement in visibility. If it is assumed that the NaCl particle-size distribution (1-5μ radius) used in these experiments is representative of that which might be produced in the field and that "proper quantities" of such particles are distributed uniformly through the lowest 100 meters of fog, the following extrapolations of these

results appear reasonable. Visibility improvements of a factor of up to three in five minutes, five in ten minutes, and 10 in fifteen minutes might be achievable under ideal conditions.

The "proper quantity" of seeding material to be used in a given fog is linearly dependent on the liquid water content of the fog. Ideally, it is that quantity of hygroscopic material that will cause redistribution of all fog liquid water without reducing the average relative humidity of the air substantially below 100%. If more than this amount of material is used, the growth rate of individual droplets formed on artificial nuclei will be retarded and total growth limited. Thus, both the rate of change of the Mie scattering coefficient due to droplet growth and the rate of decrease in liquid water content due to precipitation will be decreased.

As developed in Section III-A, the described modification of 10^8 m^3 of fog at an airport (a fog region 100 m high, 500 m wide, and 2000 m long, having a liquid water content of 200 mg m^{-3}) involves the use of approximately 90 kg of 5μ radius NaCl nuclei per seeding. The size distribution used in our experiments leads to a 65 kg mass requirement. These quantities of material are certainly feasible from an economic standpoint and seem reasonable from a corrosion standpoint.

C. Investigation of the Pre-seeding Concept

1. Results of Experiments in 8 ft^3 Cloud Chamber

Initial investigations of the concept for pre-seeding the atmosphere to prevent formation of dense radiation fog were reported in the third annual summary report (Pilié and Kocmond), 1966. Briefly, calculations indicated that optimum NaCl nucleus sizes for this purpose were in the 2 to 5μ radius region and that concentrations of 2 to 4 cm^{-3} would be sufficient to account for all liquid water made available in a radiation fog. Extensive laboratory experiments in an eight-foot tall cloud chamber showed that visibility improvements of approximately a factor of 2 could be achieved by the pre-seeding technique. Typical results of such experiments are illustrated in Figure 9 in which visibility as a function of time is compared for seeded and control fogs.

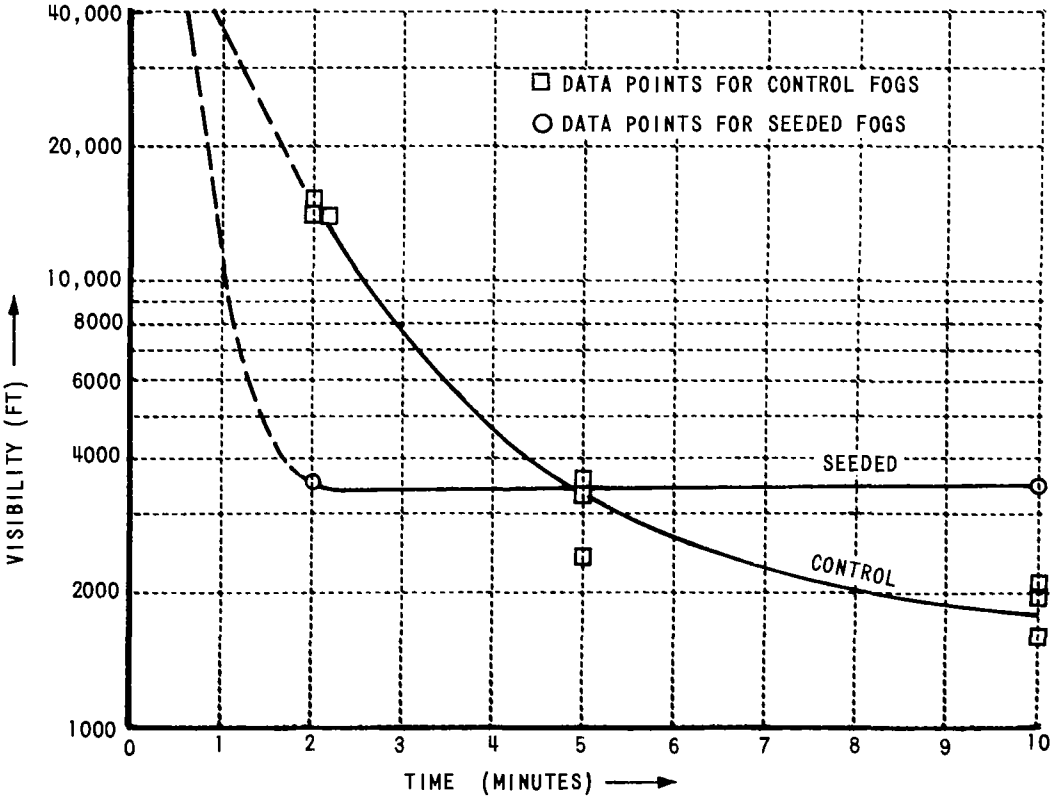

Figure 9 COMPARISON OF SEEDED AND CONTROL FOGS

The important points to be noted from the figure are: 1) the rapid, but not severe, visibility degradation in the seeded fog, and 2) the final visibility improvement (~88%) achieved from seeding.

The fact that fog forms quickly in the seeded fog is to be expected since the hygroscopic nuclei used for seeding quickly form solution drops several microns in diameter at humidities below 100%. As the drops grow and settle out of the chamber, the visibility remains essentially unchanged. In the unseeded fog, diffusional growth on natural nuclei produces a continuous degradation of visibility.

Additional experiments were conducted during the past year to determine drop sizes and concentrations in seeded and unseeded fogs. Droplet concentrations were photographically recorded with a 35 mm camera viewing an intense ribbon of light at right angles. Observations of drop size were made using gelatin-coated slide samples.

Results of measurements in the 8 ft^3 chamber show that a typically dense fog of 1000 to 1500 feet visibility (as measured by the transmissometer) consists of from 300 to 450 drops cm^{-3}. After 10 minutes of natural fog formation, drop sizes are 2 to 5μ diameter. These values of drop size and concentration are consistent with the measured attenuation, though not characteristic of radiation fog.

In seeded fog cases, after five minutes of fog formation, drop diameters usually ranged between 2μ and 25μ diameter. Drop concentrations were generally an order of magnitude less than in unseeded fogs. After ten minutes, most of the larger drops had settled out of the chamber so that drop sizes were predominantly less than 10μ. Natural fog could then begin to form and droplet concentrations slowly increased to between 300 and 400 cm^{-3}.

Having completed experiments to determine the visibility improvements that could be expected from seeding small scale laboratory fogs, the experiments were moved to the 600 m^3 chamber where more precise determination of the effects of seeding and required mass of seeding material could be made.

2. Pre-seeding Experiments in the 600 m^3 Chamber

In the pre-seeding experiments, the Ashford chamber was kept at atmospheric pressure while allowing the air to approach temperature and humidity equilibrium with the wet chamber walls. When relative humidity reached 95%, the seeding material was introduced and the near adiabatic expansion initiated. The expansion rate used was such as to produce an average cooling rate of 5^{o} C per hour during the first 15 minutes of the experiment. The sampling procedures were the same as those described earlier.

Three pre-seeding experiments were conducted in the 600 m^3 chamber. Seeding rates of 17, 8 and 4 mg NaCl m^{-3} were used. The resulting visibility improvements of the seeded fog relative to the control fog are summarized in Table VI.

Table VI

VISIBILITY IMPROVEMENT FACTOR*

PRE-FOG SEEDING			
TIME FROM START OF EXPANSION			
SEEDING MASS	+8 MIN	+12 MIN	+16 MIN
17 mg m^{-3}	(5.0) [2.0]	(2.1) [2.1]	(1.2) [1.4]
8 mg m^{-3}	(3.2) [1.7]	(3.3) [1.5]	(1.6) [1.7]
4 mg m^{-3}	(3.3) [2.1]	(3.3) [2.4]	(1.6) [1.4]

( ) INDICATE DATA FROM 15 FT LEVEL
[ ] INDICATE DATA FROM 4 FT LEVEL

* IMPROVEMENT FACTOR IS DEFINED AS THE RATIO OF THE VISIBILITY OF THE SEEDED FOG TO THE VISIBILITY OF THE CONTROL FOG AT THE SAME TIME AFTER INITIATION OF THE EXPANSION

Figure 10 shows visibility as a function of time for the experiment in which 4 mg of salt m^{-3} was injected into the chamber one-half minute before beginning the expansion. These results are typical of the three experiments. Note that at t = 0, the time at which the expansion was initiated, the visibility of the seeded fog is already substantially below that of the control fog. This initial degradation in visibility is due to the formation of droplets on artificial nuclei at subsaturated humidities. Visibility of the control fog degrades much more rapidly than that of the seeded fog after the expansion has begun.

The results of analysis shown in Figure 11 indicate that the artificial nuclei were able to condense out of the atmosphere most of the available water (even though the cooling rate during this experiment was five times as rapid as is expected in radiation fog). For the seeding rate used, the calculated concentration of artificial nuclei in the chamber was 10 cm^{-3}. Figure 11 shows that the actual concentration was 8 cm^{-3} four minutes after the expansion was started. After the same time the concentration of droplets in the control fog was 350 cm^{-3}. The liquid water content at t = 4 minutes was approximately the same in the two fogs, as indicated in Figure 11b, but the extinction coefficient per unit mass of water in the seeded fog was only one-fourth that of the control fog, as indicated in the c portion of the figure. The analysis used to obtain these data was the same as that presented in Section III. B.

As the expansion continued the solution droplets forming on artificial nuclei became too dilute to effectively compete for all water being made available by the rapid expansion, and new droplets began forming on natural nuclei. Nevertheless, at t = 7.5 minutes, even though the liquid water content of the seeded fog was approximately twice that of the control fog, the droplet concentration was only one-tenth that of the control fog and the extinction coefficient per unit mass of water was one-third that of the control fog. From that time until the end of the experiment, a combination of dilution and precipitation of large solution droplets reduced the effectiveness of the seeding and visibility in the seeded fog gradually degraded to approximately that of the control fog. The degradation was caused by a rapid increase in concentration of small droplets.

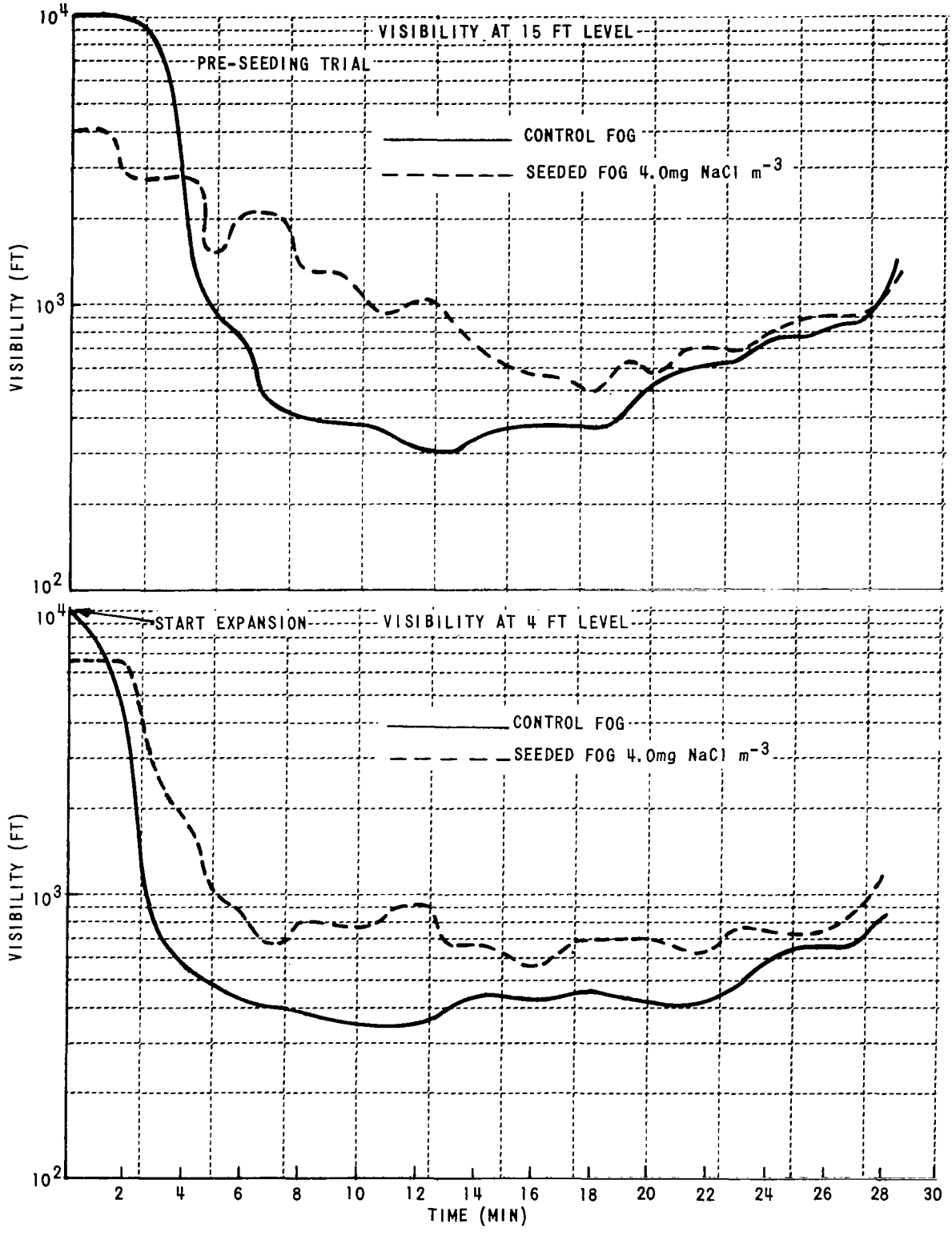

Figure 10 VISIBILITY AS A FUNCTION OF TIME FOR A SEEDED AND CONTROL FOG

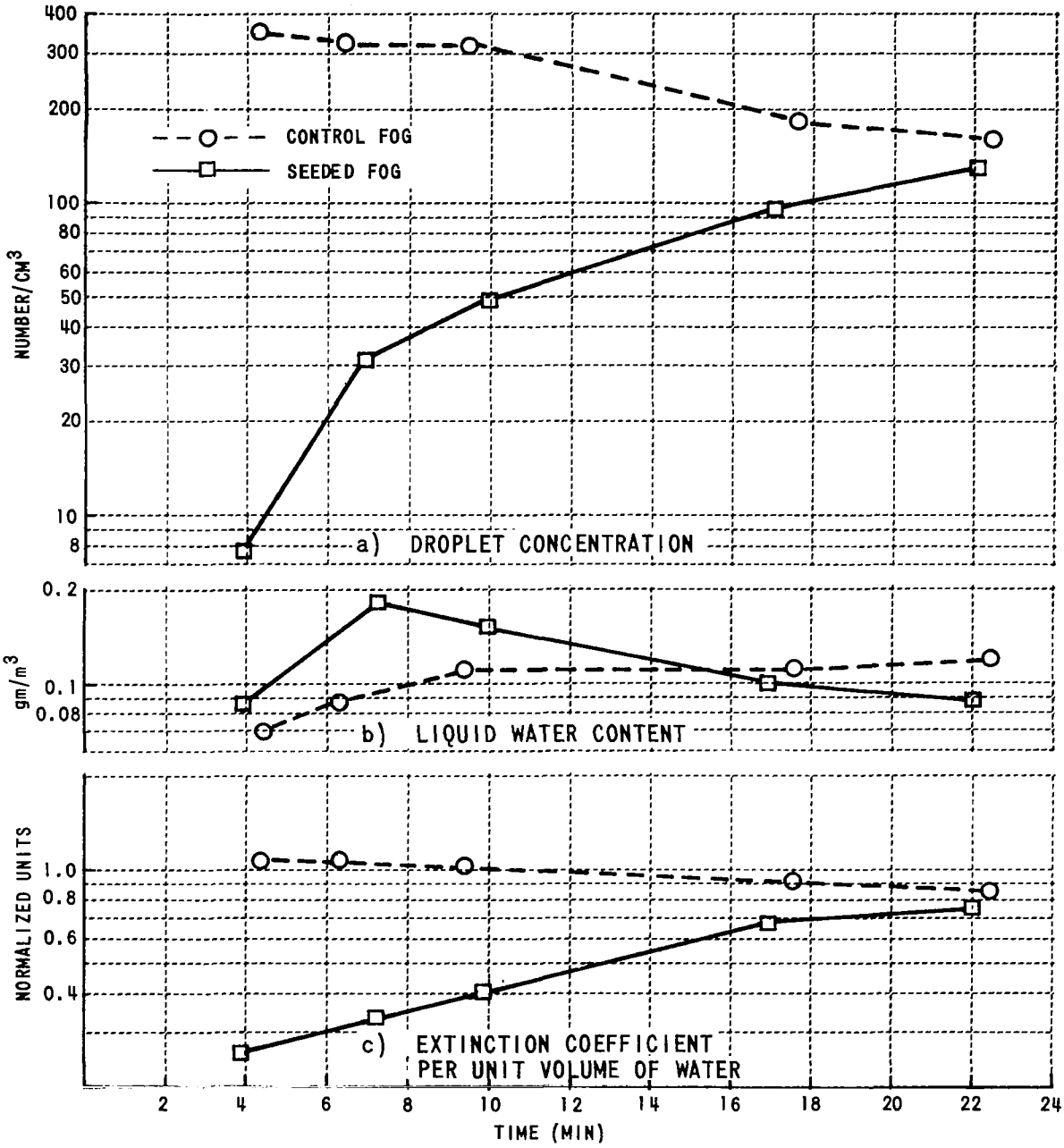

Figure 11 SEEDING RESULTS - PRE-SEEDING EXPERIMENTS

These experiments demonstrate that in principle the basic pre-seeding concept is valid and indicate that with proper procedures the severity of dense radiation fogs could be reduced. With the success of the experiments discussed in Section III-B, however, the pre-seeding concept appears to be primarily of academic interest.

D. Investigation of Atmospheric Nuclei

During the past year we have continued our investigation of atmospheric nuclei and have expanded our studies to include measurements of the concentration of nuclei that are active at subsaturated humidities. A modified thermal diffusion chamber employing saturated KNO_3 solutions was used for the latter measurements. In part 1 of this section results of this year's cloud nucleus observations are compared with data obtained during the periods 1964/65 and 1965/66. A description is given of the improved thermoelectric diffusion chamber now used for measuring concentrations of cloud nuclei. The operating principals of the "haze" chamber are discussed in part 2 along with results of initial measurements of nucleus concentrations at subsaturated humidities.

1. Cloud Nucleus Measurements

In Figure 12 a photograph is shown of the improved thermal-gradient diffusion chamber. The primary design improvement to the former chamber involved the incorporation of a thermoelectric unit (cooling module) to chill the lower water surface. In addition to improving temperature control and decreasing operation time, a considerable size and weight reduction was achieved. Moist cotton atop a porous sintered plate furnishes moisture for the upper water surface. The diameter of the plexiglass chamber is 9.8 cm and the distance between the upper and lower water surfaces is 1.7 cm. Mounted within the chamber are 10 thermocouples (five on each surface) which, in series, are used to monitor temperature differences between the upper and lower water reservoirs.

The optical system and camera used to photograph droplets at various supersaturations is the same as that used for the diffusion chamber described in the Second Annual Report No. RM-1788-P-9. Briefly, four condenser lenses and two slits collimate an intense (mercury arc) light beam and illuminate a known volume within the chamber. A polaroid camera mounted at right angles to the light beam is used to take photographs of growing droplets from which nucleus counts are made.

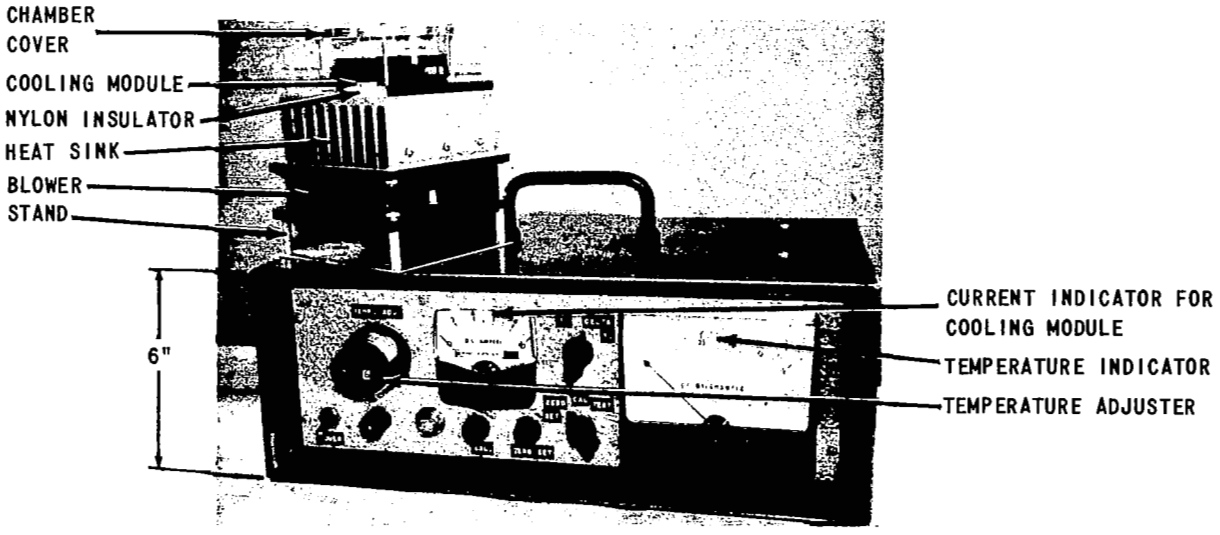

Figure 12 CAL THERMAL DIFFUSION CHAMBER AND TEMPERATURE CONTROL UNIT

In Table VII results of observations taken over a three-year period in the vicinity of Buffalo, New York are summarized and intercompared on an annual basis. The average values for all dates (shown in the last column) are representative of nucleus concentrations in an urban continental region.

TABLE VII

Average Nucleus Concentrations in Buffalo, N. Y.

Percent Super-saturation	Average for 1964/65	Average for 1965/66	Average for 1966/67	Average of all Data
3.0	5300	4100	5500	5000
1.0	3400	2600	3100	3100
0.3	1000	1000	950	1000
0.1	500	490	630	550

As reflected by the data, nucleus concentrations at 0.1% and 3.0% supersaturation during the year 1966/67 are somewhat higher than in previous years. The recent higher counts are thought to be the result of improved chamber design and observational techniques that are now used, since no particular wind direction or weather situations were found to be responsible for the elevated counts at these saturations. Note on the other hand, that at 1.0% and 0.3% supersaturation the counts are similar for all time periods.

As part of the observational routine this year, measurements of the total nucleus concentration were made with a G. E. small particle detector. This device produces supersaturations in excess of 300% (according to the manufacturer) so that all particles capable of serving as condensation sites are activated to droplet growth. Observations were tabulated according to wind direction for comparison with nucleus counts made with the thermal diffusion chamber at 0.1% supersaturation. Results are shown in Figures 13 and 14. By comparing the total nucleus content with cloud nucleus measurements, the relative importance of urbanization as a source of cloud and fog nuclei can be determined.

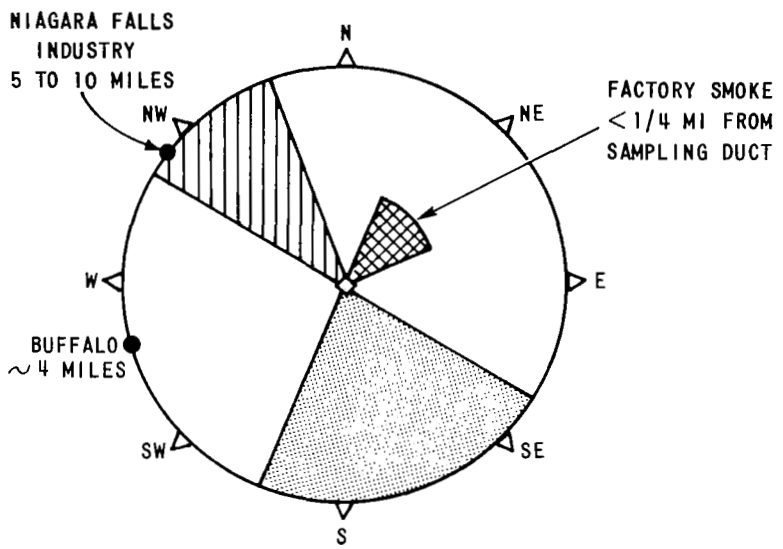

Figure 13 VARIATION IN AITKEN NUCLEUS CONCENTRATION (300% SUPERSATURATION) AS A FUNCTION OF WIND DIRECTION

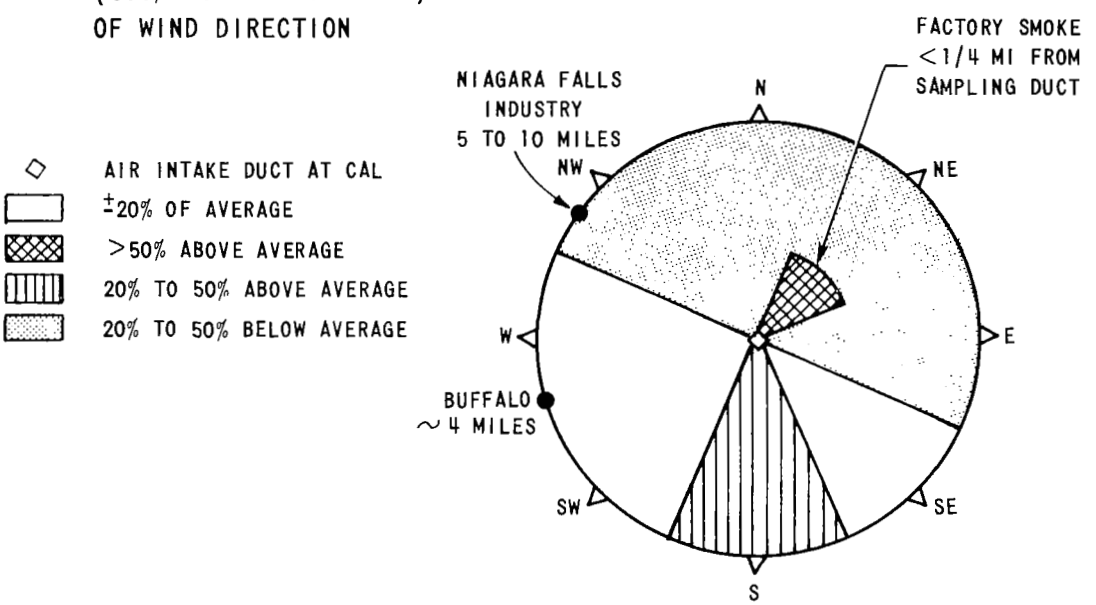

Figure 14 VARIATION IN NUCLEUS CONCENTRATION AT 0.1% SUPERSATURATION AS A FUNCTION OF WIND DIRECTION

It is obvious from the data that the correlation between Aitken nuclei and cloud nuclei is rather vague. For example, in the highly industrialized areas to the NW of CAL the total nucleus concentration is above average, as expected. To the rural south and southeast, Aitken counts are below average. The cloud nucleus population, however, is just the reverse - i.e. lower than average when winds are from the northwest and above average when they are from the south. We have suggested (Third Annual Report Summary) that the basic characteristics of the existing air mass appear most important in determining the concentration of nuclei that are active at low supersaturation. With northwest winds, for example, the cloud nucleus content at 0.1% supersaturation in relatively clean air from canadian, arctic and polar regions is not appreciably influenced by industrial areas northwest of our sampling duct. On the other hand, land sources of cloud nuclei to the south apparently play an important role in producing nuclei for cloud and fog formation. The data presented in the figures are in close agreement with the observations obtained during the time period 1964/1966 and confirm some of our previous conclusions regarding the concentration and variability of cloud nuclei.

From our measurements of cloud and fog nuclei in the Buffalo, New York area we have determined that, in general, several hundred nuclei per cm^3 are active even at 100% R.H. We suggested that a thermal gradient diffusion chamber, employing liquids other than pure water, might provide variable sub-saturation with respect to water. Such a unit could be used to investigate the concentration of large hygroscopic nuclei having relative humidity thresholds less than 100%, thereby depicting those nuclei instrumental in haze and fog formation. A review of the idea suggested that the concept was valid and that meaningful information about large ($0.1 < r < 1.0\mu$) and giant ($r > 1.0\mu$) nuclei could be obtained, using a "haze" chamber. A discussion of the haze chamber, design and operation is presented in the next section together with results of preliminary measurements. Haze chamber principals are reviewed in Appendix B.

2. The Haze Chamber - Nucleus Concentrations at Subsaturated Humidities

The basic instrument is similar in design to the improved thermal diffusion chamber discussed in part 1 of this section. Notable differences are:

a) the use of saturated KNO_3 solutions for the upper and lower water reservors.

b) a larger sensitive volume to increase total number of particles sampled. The sensitive volume of the haze chamber is 0.25 cm^3, a volume four times larger than that of the cloud chamber.

Other features of the haze chamber are essentially the same as those used for the thermal diffusion chamber (i.e. thermoelectric cooling, mercury arc illumination, polaroid photographs of droplets).

For our initial tests we chose a saturated NaCl solution since it had a base humidity (75%) of significance in atmospheric haze problems and a solubility that was nearly invariant with temperature. It was found however that very few nuclei grew to observable droplets below 95% R.H. The higher equilibrium R.H. of saturated KNO_3 solutions (94%) therefore appeared better suited for our measurements.

It should be emphasized at this point that droplet growth at subsaturated humidities is highly restrictive; that no growth can occur with nonhygroscopic nuclei and that most activated hygroscopic nuclei will do little more than deliquesce or approximately double their size. This point is illustrated in Table VIII, in which some examples of calculated droplet growth on NaCl nuclei of given size and equilibrium humidity are indicated together with the time required to achieve the indicated size.

If we assume that the minimum detectable droplet size that can be photographed in the haze chamber is about 1μ radius, then nearly all 'giant' nuclei and most 'large' nuclei can be detected at 100% R.H. At 95% R.H., on the other hand, only nuclei larger than about 0.5μ radius can be observed. Hence, a rather abrupt increase in nucleus concentration should be noted as the R.H. approaches 100%. Non-hygroscopic and Aitken nuclei are discriminated against and do not grow to observable droplet sizes at subsatured humidities.

Table VIII

DROPLET GROWTH ON NaCl NUCLEI AT
RELATIVE HUMIDITIES OF 100, 99, AND 95%

INITIAL RADIUS r	INITIAL NUCLEUS MASS	FINAL DROP SIZE AND APPROXIMATE TIME TO ACHIEVE 90% OF THIS GROWTH					
		100%R.H.		99%R.H.		95%R.H.	
		r_f	$t_{90\%r_f}$	r_f	$t_{90\%r_f}$	r_f	$t_{90\%f_r}$
0.05μ	10^{-15}g	0.3μ	<0.1SEC	0.2μ	<0.1SEC	0.15μ	<0.1SEC
0.10	10^{-14}	1.1	2.8	0.5	<1	0.3	<1
0.22	10^{-13}	3.6	92	1.1	<1	0.6	<1
0.48	10^{-12}	11.4	2780	2.5	3	1.6	<1
1.03	10^{-11}	36.1	1500 MIN	5.4	10	2.5	<1
2.23	10^{-10}	114	800 HR	11.7	30	8.0	50

3. Results of Observations

Routine haze chamber measurements have only recently been started so that statistically valid averages have not yet been established. From our measurements to date however we have discovered that there is substantial variability in haze nucleus concentrations. The nucleus spectra depicted in Figure 15 illustrates this point.

In this case study, observations of nuclei were made on two consecutive days at several relative humidities ranging from 95% to 103%. Measurements at 100% R.H. and above were obtained with the cloud nucleus chamber, while observations at subsaturation were made with the haze chamber. Between the two days of measurements a frontal passage occurred. Prior to the frontal passage winds were from the WSW. The solid curve in the figure shows that the nucleus concentration was $\sim$ 150 cm^{-3} at 95% R.H. At 100% R.H. the count was nearly an order of magnitude greater (1100 cm^{-3}).

On the following day (8/10/67) a cold front passed through the Buffalo area followed by northwest winds. Industrial effluents to the northwest caused an increase in the total particle concentration, as indicated by the counts at 3% supersaturation. Note, on the other hand, that the haze chamber counts ($<$ 100% R.H.) were nearly an order of magnitude less than the previous day. Clearly the concentrations of 'large' and 'giant' nuclei were dramatically reduced by the passage of the front. Since it is primarily these nuclei that shape the initial drop-size distribution in clouds and fog, it is likely that had a fog formed in advance of the front it would have consisted of large numbers of small drops. In the post-frontal air mass, the scarcity of suitable nuclei would suggest a fog consisting of a relatively few large drops, were one to form.

It is possible that continued measurements will provide information about the fog forming potential of an air mass and hopefully reveal useful information about sources of fog nuclei. During the coming year we expect to continue our observations of nuclei in an attempt to obtain this information.

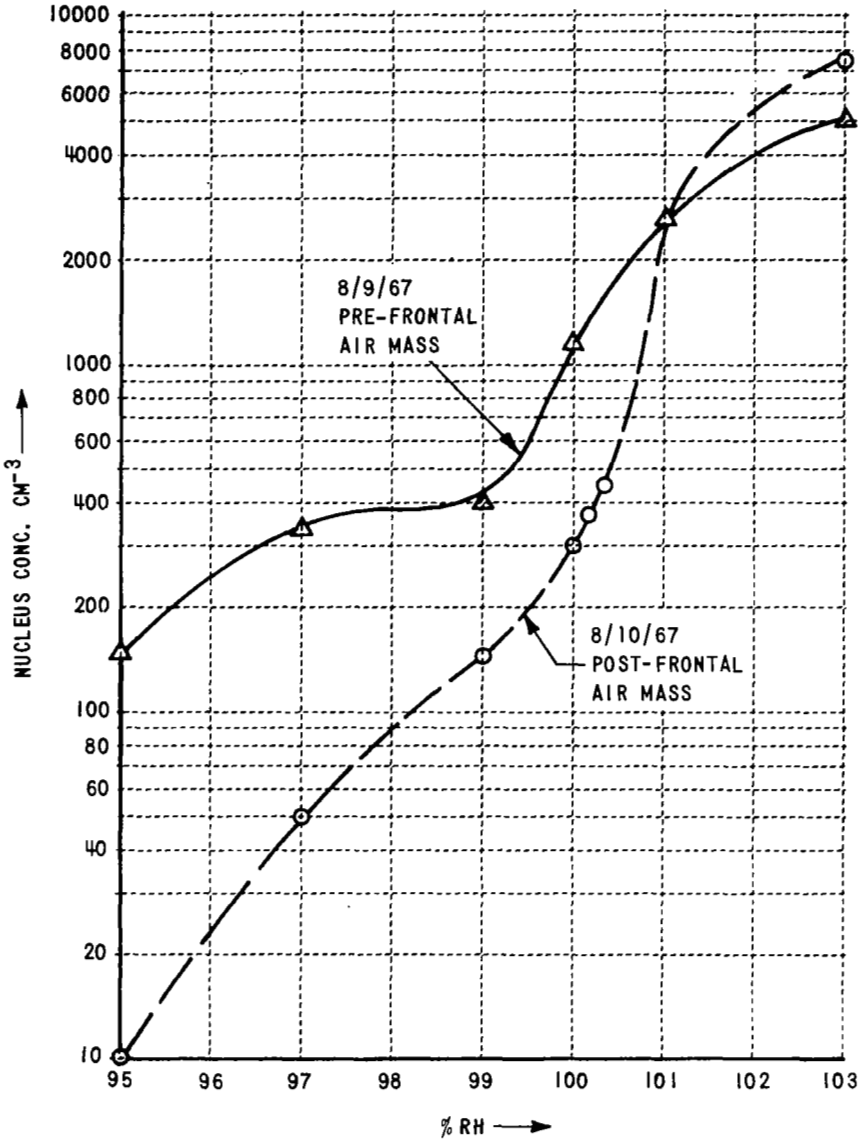

Figure 15 NUCLEUS SPECTRA BEFORE AND AFTER A FRONTAL PASSAGE

REFERENCES

Fletcher, N. H., 1962: The Physics of Rainclouds, Cambridge University Press.

Houghton, H. G. and W. H. Radford, 1938: On the Local Dissipation of Natural Fog. Papers in Physical Oceanography and Meteorology, Mass. Inst. of Tech. and Woods Hole Oceanographic Inst., Vol. VI, No. 3.

Jiusto, J. E., 1967: Nucleation Factors in the Development of Clouds, Ph.D. Dissertation in the Dept. of Meteorology, Pennsylvania State University, (Printed by the Cornell Aeronautical Laboratory, Inc.).

Pilié, R. J. and W. C. Kocmond, 1966: Project Fog Drops, Third Annual Summary Report, Cornell Aeronautical Labatory, Inc., Report No. RM-1788-P-13.

Trabert, W., 1901: Die Extinction des Lichtes in einem truben Medium (Sehweite in Wolken), Met. Z. 18, p. 518.

APPENDIX A
Particle Classifier and Disseminator Used For Fog Seeding Experiments

The device used for classifying and disseminating nuclei in our experiments is a Trost Jet Mill* which has been substantially modified on this program. A cross sectional view of the jet mill is shown in Figure 1-A. Modifications made on the mill include exit port (P_2) and the urethane insert (U) shown in the figure.

1. Operation of Trost Jet Mill Prior to Modifications

During normal operation particles are fed through the material input and travel clockwise within the classification chamber about the collector port (P_1). Compressed air or bottled gas is used to drive the mill. The two opposing gas streams cause collision and fracturing of particles in the grinding chamber. Smaller particles are removed by the cyclone action of the gas escaping through P_1. Larger particles recycle within the classification chamber until additional collisions produce finer particle sizes. The process is repeated until all of the material introduced into the mill is exhausted to the collector. The mill when used as described above, is very effective in producing sub-micron sized particles.

2. Modified Jet Mill

To produce particles in the desired size range for seeding experiments (4-10μ)** the jet mill was modified so as to include a second exit port (P_2)

---

* Manufactured by Helme Products, Inc., Helmetta, N.J.

** We have submitted a patent disclosure for the modifications made on this program.

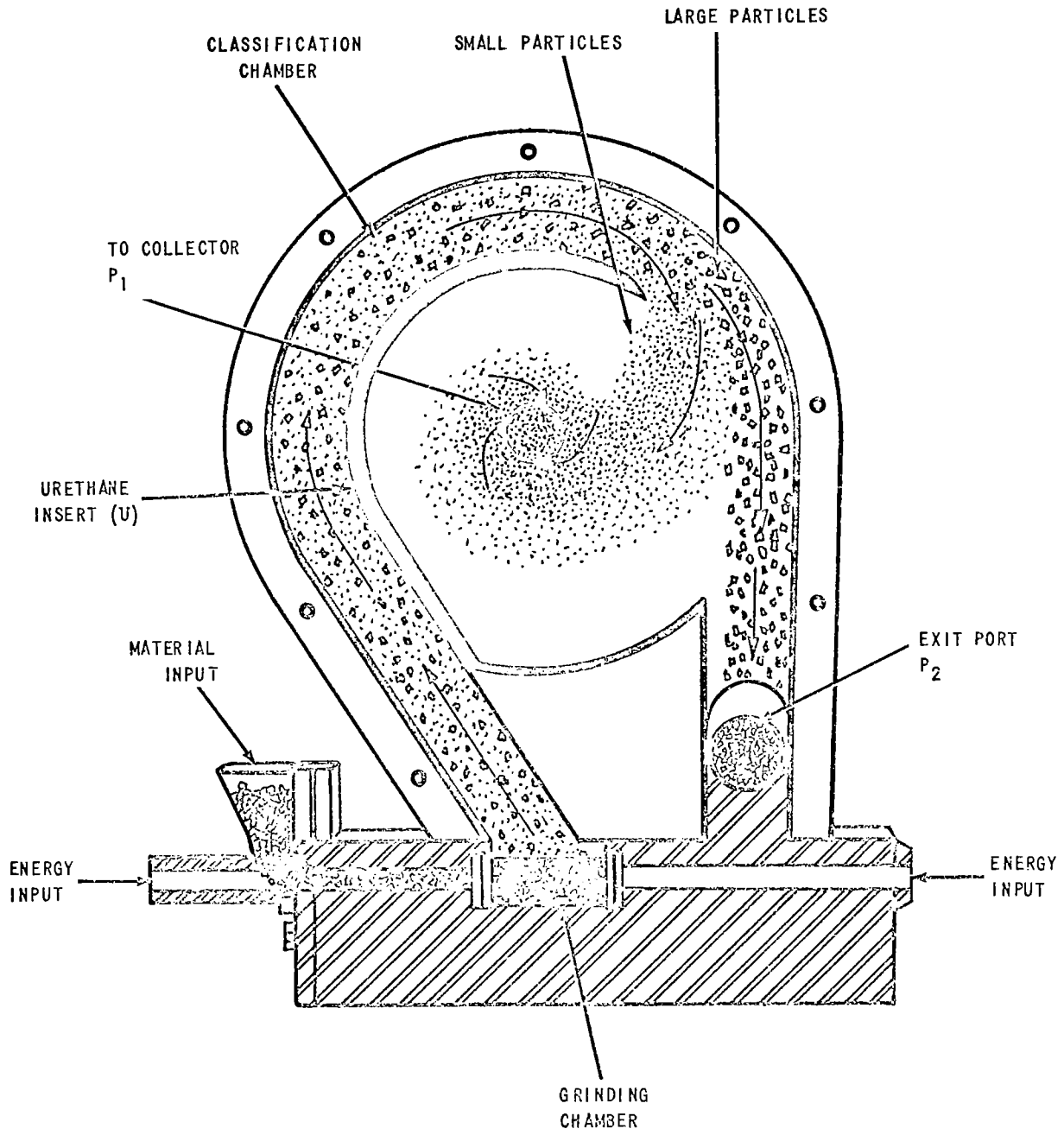

Figure 1-A TROST JET MILL WITH MODIFICATIONS

for particles. The additional port allows larger particles to be separated from the gas stream without repeated grindings, while the cyclone, or central port, is used to remove small particles in the gas stream. To further enhance particle separation a small urethane insert (U) has been installed in the classification chamber. The insert causes all incoming material to be guided about the periphery of the classification chamber until the particles approach port P_2. At that time, smaller particles having a high ratio of surface to mass, are removed by the cyclone action of the gas through P_1 and are collected in a "cyclone jar." Particles of intermediate size, which are still small enough to be undesirable, are prevented from re-entering the main particle stream by the urethane insert and are eventually drawn into P_1. Larger particles, considered desirable for seeding, are exhausted through port P_2. As a result of the aforementioned modifications we are able to produce particles in the 4-10μ size range with an efficiency of 70%, i.e. 70 percent of the particles by count are in the proper size range.

In actual operation of the mill, direct dissemination of dry salt particles into the atmosphere is possible. The modified jet mill, as described, is currently being used in our fog seeding experiments at the CAL Ordnance Laboratory, Ashford, N. Y.

APPENDIX B

Haze Chamber Principles

Aqueous salt solutions are commonly used to create fixed sub-saturated conditions in a confined environment. For ideal solutions, Raoult's Law states that the partial vapor pressure of a solution component (A) is proportional to the mole fraction of A in solution:

$$P_a = P_a^{o} \; Xa \qquad \text{or} \qquad P_a/P_a^{o} = R.H. = Xa \tag{1}$$

where $Xa = Na/_{(Na + N_b)}$, and (2)

P_a is the partial pressure of component A (water)

P_a^{o} is the vapor pressure of pure liquid A

X_a is the mole fraction of A

N_a, N_b are the number of moles of A (water) and B (salt), respectively.

Note that P_a/P_a^{o} is equivalent in this case to the relative humidity.

The relative vapor pressure lowering ΔP can be expressed as:

$$\Delta P/P_a^{o} = 1 - X_a = X_b \tag{3}$$

where X_b is the mole fraction of B (salt) present. Maximum vapor pressure lowering, corresponding to a saturated solution, varies with the salt chosen. Some examples of equilibrium humidities are given in Table 1. These humidities vary somewhat with temperature; for NaCl, the variation is only 1% over a 40^{o} temperature range (0 - 40^{o} C).

Table 1

Relative Humidity over Saturated Aqueous Salt Solutions

Temperature = 20° C

LiCl	15%
$CaCl_2 . 6H_2O$	32%
NaCl	75%
$(NH_4)_2\ SO_4$	81%
KNO_3	94%
$CaSO_4 . H_2O$	98%

Rather than using a number of separate salt solutions to simulate a range of humidity conditions, it is preferable to achieve the same versatility with a single solution. It becomes apparent that this can be done with a modified thermal-gradient diffusion chamber whose upper and lower water reservoirs are replaced with salt solution. It is essential to use identical solutions in both reservoirs and convenient if they are saturated. Figure 1 illustrates the governing principle involved.

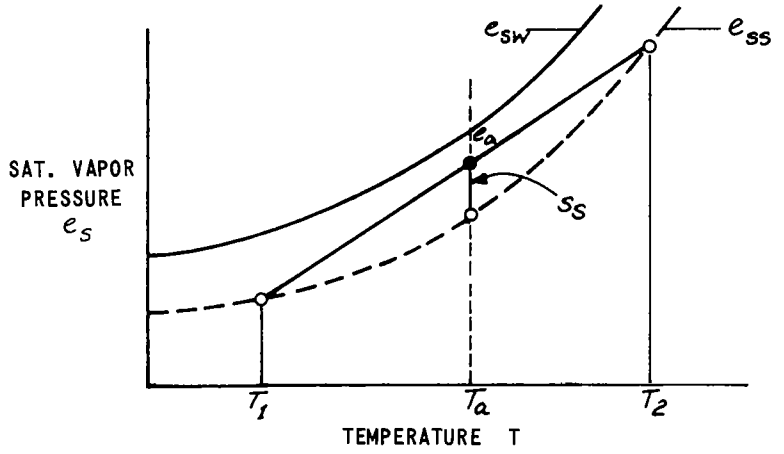

Figure 1 PHASE DIAGRAM OF HAZE CHAMBER PRINCIPLE

The solid and dashed curves represent saturation vapor pressure with respect to water and aqueous salt solution respectively. For a saturated KNO_3 solution, $e_{ss} = 0.94\, e_{sw}$. In this case with no temperature difference between reservoirs, relative humidity in the chamber is obviously 94%. As $\Delta T = T_2 - T_1$ increases, higher humidities are achieved as represented by the straight line in accordance with the following:

$$RH = 94 + 100\, S_s \tag{4}$$

$$S_s = \frac{e_a(Ta) - e_{ss}(Ta)}{e_{sw}(Ta)} \tag{5}$$

Hence, for $\Delta T = 11^{\circ}$ the relative humidity midway between the two surfaces can be computed to be 99%. Observations of nucleus concentrations above 100% R.H. can also be made with this chamber; however, because of the steep temperature gradients required to produce supersaturation, it is suggested that a thermal diffusion chamber employing plain water surfaces be used instead.

APPENDIX C

List of Symbols

a	droplet curvature term ($\sim 0.33/T$)
β	extinction coefficient
b	droplet solubility term
c	scattering factor (2.6)
E	scattering efficiency factor
g	gravitational acceleration
G	thermodynamic term
h, H	height
i	Van't Hoff factor
I	light intensity after passing through fog
I_o	light intensity in clear air
k	empirical value $1 < k < 2$
K	constant (3.91)
m_s	mass of hygroscopic nucleus
M	molecular weight of nucleus
n_r	concentration of droplets of radius r
N_i	drop concentration per unit volume
r	droplet radius
$\overline{r}$	linear-mean droplet radius

r_o	initial drop radius
r_H	final drop radius after falling distance H
RH	relative humidity
s	supersaturation
t	time
t_H	time after fall distance H
T	temperature
V	visibility
v	velocity
W	liquid water content
X	path length
ρ_o	density of drop
ρ_{air}	density of air
ρ	density of water
η	viscosity of air

NASA-Langley, 1968 —— 20 CR-1071